의학박사 학위논문

Analysis of Ventricular Remodeling in Severe Aortic Stenosis Patients

- Structural, Functional and Histologic Insights based on Multimodality Approaches -

중증 대동맥판 협착증 환자의 심실 재형성에 대한 분석

- 구조적, 기능적, 병리학적 접근에 기초한 다학제적 이해 -

2013 년 8 월

서울대학교 대학원

의학과 분자유전체의학 전공

이 승 표

A thesis of the Degree of Doctor of Philosophy in Medical Science (Molecular Genomic Medicine)

중증 대동맥판 협착증 환자의 심실 재형성에 대한 분석

- 구조적, 기능적, 병리학적 접근에 기초한 다학제적 이해 -

Analysis of Ventricular Remodeling in Severe Aortic Stenosis Patients

- Structural, Functional and Histologic Insights based on Multimodality Approaches -

August 2013

Department of Medicine

Seoul National University

College of Medicine

Seung-Pyo Lee

중증 대동맥판 협착증 환자의 심실 재형성에 대한 분석

- 구조적, 기능적, 병리학적 접근에 기초한 다학제적 이해 -

지도 교수 오 세 일

이 논문을 의학박사 학위논문으로 제출함

2013년 4월

서울대학교 대학원
의학과 분자유전체의학 전공
이 승 표

이승표의 의학박사 학위논문을 인준함

2013년 7월

위 원 장 _____ (인)
부위원장 _____ (인)
위 원 _____ (인)
위 원 _____ (인)
위 원 _____ (인)

Analysis of Ventricular Remodeling in Severe Aortic Stenosis Patients

- Structural, Functional and Histologic Insights based on Multimodality Approaches -

by

Seung-Pyo Lee

A thesis submitted to the Department of Medicine in partial fulfillment of the requirements for the Degree of Doctor of Philosophy in Medical Science (Molecular Genomic Medicine) at Seoul National University College of Medicine

July 2013

Approved by Thesis Committee:

Professor _____ **Chairman**

Professor _____ **Vice chairman**

Professor _____

Professor _____

Professor _____

ABSTRACT

Introduction: Aortic stenosis (AS) is increasing worldwide and in Korea. Silent myocardial damage and fibrosis is common and therefore, detection of even subtle myocardial remodeling may be important for understanding the disease process and to establish an evidence-based treatment guideline.

Methods: This series of analysis is based on a prospective cohort of moderate to severe AS patients. The patients in cohort 1 were severe AS patients with normal ejection fraction (EF) and divided into paradoxical low-flow (PLF-AS) and normal-flow AS (LF-AS) patients. Global longitudinal/circumferential strain (GLS/GCS) measured by 2D-speckle tracking imaging were compared between the two groups. The patients in cohort 2 underwent 2-dimensional echocardiography and cardiac magnetic resonance (CMR). The correlation between late gadolinium enhancement (LGE), EF and various LV functional parameters was analyzed. The patients in cohort 3 were severe AS patients with normal LVEF undergoing aortic valve replacement and endomyocardial biopsy. The specimens were stained with platelet-endothelial cell adhesion molecule-1 to investigate the correlation between myocardial vessel density and various echocardiographic parameters. Finally, minimally symptomatic moderate or severe AS patients with normal LVEF were enrolled in cohort 4. All underwent CMR including modified Look-Locker Inversion recovery sequence and the native T1 values were compared with various parameters of LV remodeling.

Results: In patients enrolled to cohort 1, PLF-AS patients showed significantly impaired GLS in spite of preserved LVEF and the global LV afterload, represented by valvuloarterial impedance, was a significant determinant of GLS. In the patients enrolled to cohort 2, there was a significant trend towards adverse structural and functional remodeling in severe AS patients if there was either LGE or LV systolic dysfunction on CMR. Also, even if the LVEF was normal, those with LGE on CMR had significantly stiffer LV compared with those without. Analysis of the data from patients in cohort 3 revealed that the degree of myocardial angiogenesis correlates well with both LV systolic/diastolic function and the degree of LV hypertrophy. Also, there was a trend towards more myocardial angiogenesis with worsening of the LV geometry. Finally, in patients from cohort 4, native T1 value reflected the diffuse myocardial fibrosis degree and even in patients with minimal symptoms, patients with more diffuse myocardial fibrosis demonstrate a progressed degree of subclinical ventricular remodeling that was not reflected by the symptomatic status of the patient.

Conclusion: These findings demonstrate that using 2D-speckle tracking imaging with echocardiography, LGE and native T1 with CMR, it may be possible to detect the subtle ventricular structural and functional remodeling in patients with severe AS, even those with normal LVEF. In addition, there seems to be a compensatory angiogenic process in the myocardium with worsening of the AS degree. These findings warrants further in-depth investigations into the process of LV remodeling in patients with severe AS and how it is related to patient outcome.

*The result from patients in cohort 1 is published in the Journal of the American Society of Echocardiography (J Am Soc Echocardiogr. 2011;24(9):976-83.).

Keywords (in alphabetical order): Angiogenesis, Aortic stenosis, Cardiac magnetic resonance, Echocardiography, Ventricular remodeling

Student number: 2009-31103

CONTENTS

LIST OF TABLES AND FIGURES

Chapter 1

Chapter 2

Chapter 3

Chapter 4

LIST OF ABBREVIATIONS

2D-STI; 2D-speckle tracking imaging

AS; Aortic stenosis

AVA; Aortic valve area

AVR; Aortic valve replacement

BSA; Body surface area

CMR; Cardiac magnetic resonance

DE/LGE; Delayed/late gadolinium enhancement

Ed/Ees; Diastolic/end-systolic elastance

EF; Ejection fraction

GCS/GLS; Global circumferential/longitudinal strain

LV(OT); Left ventricle/ventricular (outflow tract)

NF-AS/PLF-AS; Normal/paradoxical low flow-aortic stenosis

NYHA; New York Heart Association

PECAM-1; Platelet endothelial cell adhesion molecule-1

PG; Pressure gradient

RWT; Relative wall thickness

SD; Standard deviation

SBP/DBP; Systolic/diastolic blood pressure

SV(i); Stroke volume (index)

TE/TR; Excitation time/Relaxation time

TVI; Time velocity integral

Z_{va}; Valvuloarterial impedance

GENERAL INTRODUCTION

Aortic stenosis (AS) is an increasing valvular heart disease not only in the Westernized countries but also in Korea. It typically provokes pressure overload to the left ventricle, leading to an initial stage of left ventricular hypertrophy, fibrosis and diastolic problems. After this initial stage, systolic problems of the left ventricle starts and therefore, the current guidelines recommend that surgical repair of the aortic valve should be done before this systolic dysfunction.

With the advances of various imaging techniques, it has become more and more easier to analyze and visualize the anatomical and functional remodeling of the heart. Specifically, subtle functional problems of the ventricle can be analyzed using speckle tracking imaging with echocardiography. Also, very minute damage of the ventricle can also be visualized using late gadolinium enhancement (LGE) with cardiovascular magnetic resonance (CMR). The clinical utility of these techniques has provided insight into the understanding of the role of these modalities in aortic stenosis patients.

However, before judging whether newer imaging modalities can be integrated into a daily part of clinical decision, it would be absolutely necessary to test whether these modalities are in fact sensitive in predicting subtle changes in the myocardium. Although there have been a few papers suggesting an additive role of these modalities in severe AS patients, the role of speckle tracking imaging and CMR in severe AS patients remains yet to be verified. In addition, the pathological process undergoing left ventricular

hypertrophy in various animal models has to be verified in severe AS patients so that these process can be translated into a novel diagnostic and therapeutic mean.

Therefore, the series of work in this thesis includes a variety of my efforts to unveil the possible application of new imaging modalities and also, to suggest a possible mechanism in the ventricular remodeling in severe AS patients. The findings here demonstrate that indeed speckle tracking imaging with echocardiography and LGE with CMR can predict the remodeling of the ventricle in severe AS and that compensatory angiogenesis may underlie the pathogenesis involved in this process. Also, native T1 values using the MOLLI sequence with CMR may shed light into the quantification of diffuse myocardial fibrosis.

CHAPTER 1

Deterioration of Myocardial Function in Paradoxical Low-Flow Severe Aortic Stenosis : 2-Dimensional Strain Analysis

INTRODUCTION

Current ACC/AHA guidelines recommend the following Doppler measurements as the diagnostic criteria for severe aortic stenosis (AS); aortic valve area (AVA)<1.0cm^2 and/or AVA index<0.6cm^2/m^2, transaortic mean pressure gradient (PG)>40mmHg and peak velocity>4.0m/s(1). However these criteria have been challenged with recent reports of paradoxical low-flow, low-gradient AS, which do not meet the forementioned criteria of severe AS(2). To make matters more perplexing, paradoxical low-flow severe AS (PLF-AS) patients carry a worse prognosis if treated medically and yet, the proportion of patients getting the right diagnosis and timely operative correction is significantly lower than that in patients with normal-flow severe AS (NF-AS)(3). Therefore, correct diagnosis and identification of PLF-AS is important to improve the clinical outcome. In this regard, the pathophysiology of PLF-AS needs to be clarified.

It is well known that impaired left ventricular (LV) myocardial function is an important determinant of clinical outcome in AS. Accordingly, we hypothesized that LV myocardial function is deteriorated and may lead to poor clinical outcome in PLF-AS. We also hypothesized that global afterload on LV is an important determinant of LV dysfunction in these patients. We used 2-dimensional global strain based on speckle tracking imaging (2D-STI) because it is useful for assessing the multidirectional myocardial mechanics, relatively independent of the loading conditions, and also a useful prognostic factor of various conditions of the heart(4, 5).

MATERIALS AND METHODS

1. Patient population

A total of 103 patients with severe AS and preserved LV ejection fraction (EF) (>50%) per definition of AVA<1.0cm^2 in the ACC/AHA guideline were enrolled in the study irrespective of the symptom status. Patients with significant concomitant valvular heart disease of grade 3 or more other than AS i.e. concomitant aortic regurgitation or mitral/tricuspid/pulmonic valve disease, significant regional wall motion abnormality or history of myocardial infarction or previous cardiac surgery were excluded. PLF-AS was defined as stroke volume index (SVi)<35mL/m^2 according to previous literature(2) and NF-AS was designated otherwise (**Figure 1**). All patients gave informed consent to the study, the protocol of which was approved by the Institutional Review Board of Seoul National University Hospital. Baseline laboratory tests, anthropometric measures and medical history were taken at the time of echocardiographic examination.

2. Two-dimensional echocardiography

All patients underwent comprehensive 2D-echocardiographic examination using a 3.5MHz transducer in a commercially available equipment (Vivid 7, GE Medical System, Horten, Norway). LV end-diastolic/systolic diameters and wall thickness were measured using standard M-mode tracings at the parasternal short-axis view of papillary muscle level and the ejection fraction calculated by these M-mode measurements. Relative

wall thickness (RWT) was estimated by calculating the following; RWT=2×(Diastolic LV posterior wall thickness)/(LVIDd), where LVIDd is the LV internal diastolic dimension. The dimensions of the aortic root, i.e. LV outflow tract (LVOT), sinotubular junction and ascending thoracic aorta diameter were measured at the standard parasternal long-axis view. End-diastolic and systolic volumes were obtained with the modified biplanar method at apical four and two-chamber views. LV mass index (LVMI) was calculated with the following formula: (1.05×[(LVIDd+diastolic LV posterior wall thickness+diastolic ventricular septal thickness)^3–LVIDd^3]-13.6)/BSA, where 1.05 is the specific gravity of the myocardium(6). Peak early (E) and late (A) diastolic velocity of mitral inflow and peak early (E') and late (A') diastolic mitral annulus velocity at the septal side were measured in apical four-chamber view. All echocardiographic measurements were averaged for three beats for patients in sinus rhythm and five beats in atrial fibrillation with baseline heart rate of <100BPM.

Time velocity integral (TVI) of the LVOT was measured at apical five-chamber view and stroke volume (SV) was calculated with LVOT area (0.785 x (LVOT diameter)^2) multiplied by TVI at the LVOT. SVi was calculated by dividing SV with body-surface area (BSA), which in turn was calculated using the Mostella formula. AVA was calculated using the continuity equation (TVI at AV/(TVI at LVOT x LVOT area)) and indexed by AVA/BSA. Mean transaortic pressure gradient (PG) was estimated by manual tracing of the flow velocity using continuous-wave Doppler recordings at apical five-chamber view. Valvuloarterial impedance (Z_{va}) was calculated according to

the following formula; (systolic blood pressure (SBP)+transaortic mean PG)/SVi(2).

3. 2D speckle tracking imaging analysis

Digital loop image was obtained at the most optimal frame rate (50~100 frame/second), sector width and image depth at an end-expiratory breath-hold from parasternal short-axis view at the papillary muscle level and apical views. All images were taken without a dual-focusing tool to obtain high frame rate adequate for speckle tracking imaging. LV endocardial border was traced at end-systolic frame and the region-of-interest was defined automatically by the off-line analysis program (EchoPac 5.0.1 for PC, GE Medical System) between the endocardial and epicardial borders. Myocardial tracking was verified, and the region-of-interest width was adjusted to optimize the tracking, if needed. Care was taken to ensure at least five segments were tracked adequately from each plane to get an adequate global strain measure. Strain curve was obtained by a single independent observer blinded to the objective of the study. Peak global circumferential/longitudinal strain value was defined as the peak negative value of the strain curve in a single beat cardiac cycle and calculated for the entire circular/U-shaped LV myocardium as follows; global strain=(L[end-systole]–L[end-diastole])/L[end-diastole]×100(%) (L, whole LV myocardium as one big segment)(7), where global strain is the myocardial deformity of the myocardium as a whole and not an average of each segmental strain as in previous literatures concerning average strain in severe AS patients(8, 9). Peak global circumferential strain

(GCS) was measured at midventricular parasternal short axis view, whereas global longitudinal strain (GLS) at apical two, four and three chamber views and averaged(4).

4. Statistical Analysis

Continuous or dichotomous variables are presented as mean±SD or percentages and compared using Student's t-test or $\chi 2$-test, respectively. Bivariate correlation analysis was drawn between GLS/GCS and SVi, Z_{va}, indexed AVA and E/E'. The degree of correlationship is presented as Pearson's correlation coefficient. Variables that were considered related to myocardial function were initially analyzed with univariable analysis and then, variables with a p-value<0.1 were incorporated into the generalized linear model (GLM) to identify significant factors associated with GLS. In this process, some variables were also analyzed for multicolinearity and those shown to be interrelated were omitted for final multivariate analysis. All analysis was done with SPSS version 17.0 (SPSS Inc., Chicago, IL) and two-tailed p-value of <0.05 was considered statistically significant.

RESULTS

Among 103 patients, 16 patients were classified as PLF-AS. PLF-AS patients tended to have bigger BSA, less likely to have hypertension and more likely to have atrial fibrillation (**Table 1-1**). Interestingly, the PLF-AS patients also tended to be in a worse functional status compared with NF-AS patients (average NYHA functional capacity 1.96±0.62 for NF-AS patients vs. 2.38±0.70 for PLF-AS patients, p-value=0.02).

Compared with NF-AS group, LVEF was significantly lower in PLF-AS group, which was partially explained by larger end-systolic dimension/volume. Of note, the PLF-AS groups also tended to have thicker myocardium, as shown by significantly thicker interventricular septum and posterior wall, and also, a tendency towards concentric remodeling shown by RWT, compared with NF-AS group. Although there was no difference in the aortic root dimensions between the two groups, the AVA or indexed AVA was significantly smaller in the PLF-AS group. These results are summarized in Table 1-2. Intriguingly, a significantly worse GLS was observed in the PLF-AS group (**Figure 1-1**) although there was no difference in the GCS. In addition, valvuloarterial impedance (Z_{va}), a parameter of global LV afterload, was significantly increased in PLF-AS group.

By bivariate correlation analysis, there was a significant negative correlationship between SVi and GLS and also, between SVi and GCS (r=-0.324, p=0.001 for GLS, r=-0.244, p=0.024 for GCS) (**Figure 1-2A and B**). Valvuloarterial impedance showed good positive correlationship with GLS

	Total (n=103)	NF-AS (n=87)	PLF-AS (n=16)	p-value
Age (year)	67.5±9.7	67.2±10.2	69.2±6.8	0.34
Male (%)	60.2 (62)	58.6 (51)	68.8 (11)	>0.99
BSA (m^2)	1.66±0.17	1.64±0.17	1.77±0.18	0.02
Diabetes mellitus (%)	26.2 (27)	27.6 (24)	18.8 (3)	0.55
Hypertension (%)	50.5 (52)	54.0 (47)	31.2 (5)	0.09
Systolic BP (mmHg)	129±18	130±19	120±9	0.01
Diastolic BP (mmHg)	71±10	71±10	71±10	0.86
Current smoker (%)	9.7 (10)	9.2 (8)	12.5 (2)	0.65
Hyperlidemia (%)	11.7 (12)	12.6 (11)	6.2 (1)	0.69
NYHA functional status	2.03±0.65	1.96±0.62	2.38±0.70	0.02
Atrial fibrillation (%)	6.8 (7)	4.6 (4)	25.0 (4)	0.02
Baseline Cr (mg/dL)	1.07±0.43	1.07±0.46	1.10±0.29	0.82
Bicuspid AV (%)	46.6 (48)	42.5 (37)	68.8 (11)	0.05
Operation (%)	61.2 (63)	56.3 (49)	87.5 (14)	0.02

Table 1-1. Baseline clinical characteristics of the study participants.

NF-AS, normal flow aortic stenosis; PLF-AS, paradoxical low flow aortic stenosis; BSA, body-surface area; NYHA, New York Heart Association.

	Total (n=103)	NF-AS (n=87)	PLF-AS (n=16)	p-value
LVEDD (mm)	49.4±4.9	49.3±5.0	49.6±4.2	0.82
LVESD (mm)	30.2±4.6	29.9±4.7	32.1±4.2	0.08
LVEDV (mL)	108.9±31.5	107.5±29.3	116.5±41.6	0.30
LVESV (mL)	41.3±16.9	39.6±15.4	49.9±22.0	0.09
LVEF (%)	62.6±7.2	63.5±6.7	57.5±7.7	<0.01
IVS (mm)	12.1±2.2	11.9±2.0	13.4±2.9	0.02
PW (mm)	11.6±2.3	11.4±2.1	12.9±2.8	0.01
E (m/sec)	0.78±0.29	0.78±0.29	0.79±0.31	0.91
A (m/sec)	0.90±0.27	0.91±0.26	0.85±0.36	0.42
DT (msec)	245±79	248±80	224±78	0.29
E' (cm/sec)	4.7±1.7	4.8±1.7	4.1±1.8	0.17
A' (cm/sec)	7.0±2.0	7.1±2.1	6.2±1.3	0.14
E/E'	18.8±10.0	18.4±10.4	20.9±7.6	0.36
Vmax (m/sec)	4.6±0.8	4.6±0.8	4.3±0.8	0.19
AVA (cm^2)	0.74±0.20	0.78±0.19	0.53±0.15	<0.01
AVAi (cm^2/m^2)	0.45±0.12	0.47±0.10	0.30±0.10	<0.01
Mean PG (mmHg)	51.1±20.5	51.9±21.4	46.6±14.2	0.34
Z_{va} ($mmHg \cdot m^2/mL$)	3.96±1.17	3.65±0.83	5.62±1.33	<0.01
GLS (%)	-15.8±4.3	-16.4±4.0	-12.6±4.4	<0.01

GCS (%)	-17.7±4.6	-18.0±4.6	-16.1±4.9	0.17
LVMI (g/m^2)	174.6±51.6	171.5±49.6	191.0±59.9	0.17
RWT	0.48±0.10	0.47±0.09	0.52±0.12	0.03

Table 1-2. Baseline echocardiographic parameters of the study participants.

LVEDD/LVESD, left ventricular end-diastolic/systolic dimension; LVEDV/LVESV, left ventricular end-diastolic/systolic volume; IVS, interventricular septum thickness; PW, posterior wall thickness; E/ A, peak early (E) and late (A) velocity at mitral inflow; DT, deceleration time; E'/A', peak early (E') and late (A') mitral annulus velocity; Vmax, maximal transaortic velocity; AVAi, aortic valve area index; mean PG, mean transaortic pressure gradient; Z_{va}, valvuloarterial impendace; GLS/GCS, global longitudinal/circumferential strain; LVMI, LV mass index.

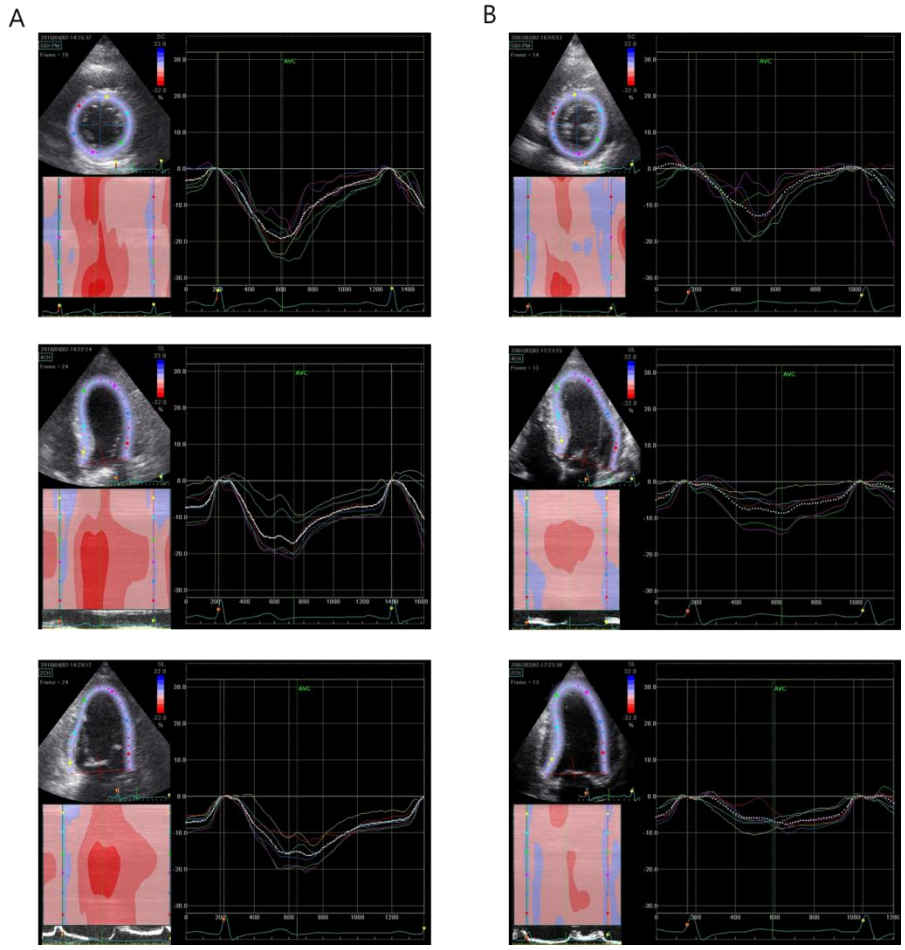

Figure 1-1. Representative color Doppler and strain images of normal flow-aortic stenosis (NF-AS) and paradoxical low flow-aortic stenosis (PLF-AS).

(A) Representative 2D-speckle tracking images of NF-AS. Stroke volume index was 53.9mL/m^2 and AVA 0.80cm^2. The global strain was GLS -17.2%, GCS -19.2%.

(B) Representative 2D-speckle tracking images of PLF-AS. Stroke volume index was 30.3mL/m^2 and AVA 0.42cm^2. The global strain was GLS -8.9%, GCS -12.4%.

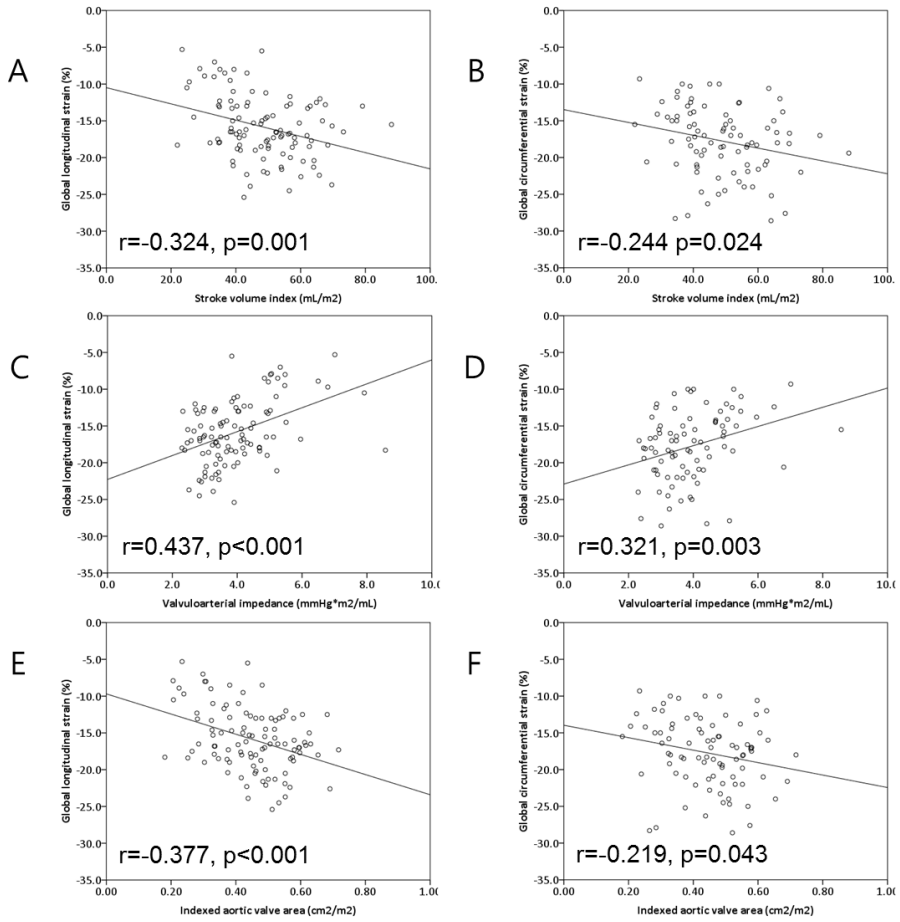

Figure 1-2. Correlation between global strain and stroke volume index, valvuloarterial impedance

(A, B) Negative correlation between global longitudinal/circumferential strain and stroke volume index.

(C, D) Positive correlation between global strain and valvuloarterial impedance. Slightly stronger correlation was observed with global longitudinal strain compared with circumferential strain.

(E, F) A significant negative correlation was observed between global longitudinal strain and indexed aortic valve area (E), in contrast to marginal

correlation with global circumferential strain (F). r, Pearson's correlation coefficient.

(r=0.437 p<0.001 for Z_{va} and GLS, **Figure 1-2C**) and also GCS, albeit at a lesser degree (r=0.321, p=0.003 for Z_{va} and GCS, **Figure 1-2D**). GLS also showed significant negative correlationship with AVA index (r=-0.377 for indexed AVA and GLS, p-value<0.001). GCS marginally correlated with AVA index (r=-0.219 for indexed AVA and GCS, p-value=0.043) (**Figure 1-2E and F**).

To analyze the correlationship of global strain with known echocardiographic predictors of clinical outcome, correlation was analyzed between GLS and E/e'. Positive correlationship existed between E/E' and GLS (r=0.367, p<0.001 for E/E' and GLS, **Figure 1-3A**) and also, between E/E'and valvuloarterial impedance (r=0.207, p=0.037 for E/E'and Z_{va}, **Figure 1-3B**).

Factors considered to be associated with myocardial function/deformation in severe AS, including sex, age, diabetes, hypertension, serum creatinine, mean transaortic PG, AVA, global LV afterload and maximal transaortic velocity were analyzed using the GLM model. Among these factors, age, serum creatinine, mean transaortic PG, AVA, global LV afterload and maximal transaortic velocity all turned out to be significantly associated with GLS. However as mean transaortic PG, AVA, valvuloarterial impedance and maximal transaortic velocity were interrelated with each other significantly (multicolinearity), only valvuloarterial impedance entered the final multivariable analysis. In final, only age and valvuloarterial impedance were significant determinants of GLS (**Table 1-3**).

Finally, we collected data on outcome of these patients by defining adverse

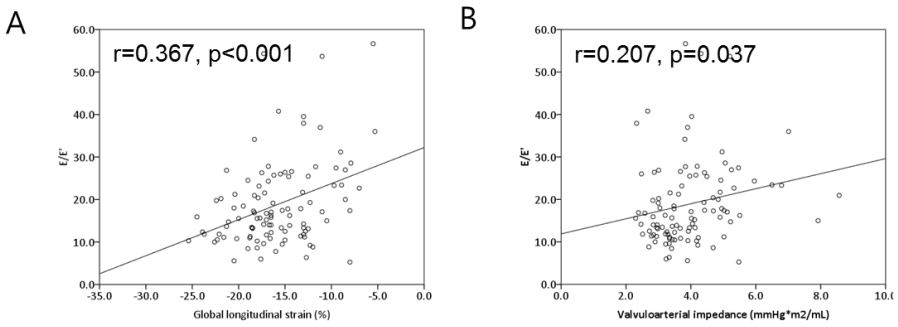

Figure 1-3. Correlation between E/E' and global longitudinal strain, valvuloarterial impedance.

A significant positive correlation was observed between E/E' and global longitudinal strain (A) and valvuloarterial impedance (B). r, Pearson's correlation coefficient.

	Univariable analysis		Multivariable analysis	
	β (95% CI)	p-value	β (95% CI)	p-value
Male	0.06 (-0.34~0.45)	0.77		
Diabetes mellitus	-0.30 (-0.74~0.14)	0.18		
Hypertension	0.33 (-0.06~0.72)	0.10		
Atrial fibrillation	-0.57 (-1.29~0.16)	0.13		
Smoking	-0.34 (-0.99~0.32)	0.31		
Hyperlipidemia	0.33 (-0.27~0.93)	0.28		
Age	0.10 (0.08~0.12)	<0.01	0.07 (0.05~0.09)	<0.01
Serum Cr	0.70 (0.25~1.16)	<0.01	0.31 (-0.15~0.76)	0.19
Aortic valve area	-7.69 (-8.64~-6.73)	<0.01		
Mean transaortic PG	0.03 (0.02~0.04)	<0.01		
Peak transaortic velocity	-0.59 (-0.82~-0.35)	<0.01		
Valvuloarterial impedance	1.63 (1.46~1.79)	<0.01	1.53 (1.37~1.70)	<0.01

Table 1-3. Predictors of global longitudinal strain among AS severity parameters by generalized linear model.

Aortic valve area, mean transaortic PG and peak transaortic velocity have been omitted from multivariable analysis for global longitudinal strain because of multicolinearity between these factors and valvuloarterial impedance. Cr, creatinine; PG, pressure gradient.

outcomes as cardiovascular death, stroke, AVR operation and worsening of functional capacity to NYHA functional class III or IV. Although marginal, PLF-AS patients had more events compared with NF-AS patients (93.8% (15/16) in PLF-AS patients vs. 69.8% (60/87) in NF-AS patients, $\chi 2=3.99$, p=0.063). Also, to eliminate the possibility of AVR as a strong bias factor and also, to show that strain may be a prognostic factor, we collected data from those who did not undergo or refused AVR (n=40). This group of population was analyzed for cardiovascular death and worsening of functional capacity to NYHA functional class III or IV to see the natural course of severe AS. Compared with 28 patients without events, 12 patients with events had significantly worse GLS (-16.5±3.2 for patients without events vs. -12.6±4.2 for patients with events, p=0.01).

DISCUSSION

The main finding of this study is that (1) PLF-AS patients showed significantly impaired myocardial function in spite of preserved LVEF as verified by GLS with the use of 2D-STI, (2) global LV afterload, represented by valvuloarterial impedance, may be a significant determinant of subclinical LV dysfunction in severe AS and (3) GLS might be useful to corroborate the diagnosis PLF-AS and also to predict the prognosis of severe AS.

Global strain for analysis of myocardial function in severe AS

Global strain has been demonstrated to be useful for assessing myocardial function(4, 10). It is simple to analyze, reproducible and technically feasible. It is less affected by geometrical characteristics as compared to LVEF(11). Most importantly, it is more sensitive to detect subtle myocardial dysfunction in certain conditions(12) thanks to its capability of multidirectional analysis. We believe that these advantages are very important in valvular heart disease, in which significant changes in volume status and LV geometry may occur(13).

GLS was significantly impaired in patients with PLF-AS, which is suggestive of subendocardial dysfunction or may be pathological changes in the myocardium such as myocardial fibrosis. Most importantly, there have been previous reports demonstrating that increased afterload(14-16) leads to decrease of LV strain. Also, these reports have consistently suggested that increased afterload results in longitudinal LV dysfunction and this may be due

to the fact that subendocardial fibers are arranged in a longitudinal manner which results in a significant increase in the wall stress compared with the circumferentially arrayed midwall fibers(17). In addition, there have also been reports demonstrating the distribution of myocardial fibrosis mainly at the subendocardium, with the degree of fibrosis correlating with Doppler-derived strain imaging(18) and also, long-term survival(19). Therefore, the increased afterload, which may be the main mechanism and possibly, the profibrotic milieu may be a plausible explanation of significantly depressed GLS but not GCS in our AS patients, in particular PLF-AS patients, which is in line with previous findings(8, 20, 21). In contrast to GLS, there have been conflicting results regarding GCS and radial strain in PLF-AS. Lancellotti et.al reported that PLF-AS patients showed significantly worse GCS and radial strain compared with NF-AS group(9). In contrast, others have demonstrated that there may be a significant decrease of longitudinal strain but not radial strain in severe AS(14, 16, 18, 20). These difference are likely due to the differences in the severity of AS and myocardial dysfunction of the study population.

Global strain as a guide for diagnosis and estimating prognosis of PLF-AS

According to the results of this study, GLS may also be useful for the diagnosis of PLF-AS and identification of those who need surgery. These patients tend to have worse cardiac function, i.e. smaller stroke volume, which may partly be explained by more hypertrophic myocardium and also, smaller LV dimensions, the analysis of which has been verified in our data and also in

other data as well(2, 20). Therefore, proper detection of PLF-AS is important because it carries a poor prognosis and a substantial proportion of these patients can be saved with timely operation(2, 3). Currently, diagnosis of PLF-AS relies solely on Doppler measurements such as transaortic mean PG, AVA and SVi, that are prone to errors in clinical practice. Even the experienced physicians are confused when these parameters are not in accord, and therefore physicians are apt to delay corrective operation for those who are most in need of these measures(3). In the seminal work by Hachicha et al, PLF-AS patients were more likely to have decreased LVEF, stroke volume and cardiac output/index, all predicting towards a myocardial contractile dysfunction and subsequently, poorer prognosis. However, these parameters may not correctly reflect the intrinsic myocardial performance, which is in contrast to our analysis with global strain. Of note, Clavel and Pibarot et.al. have suggested the efficacy of projected AVA using dobutamine stress echocardiography for prediction of AS severity in patients with decreased LV ejection fraction recently(22). Although the exact cut-off value and the diagnostic accuracy remain to be confirmed in a larger study, the efficacy of strain for the diagnosis(9) and risk stratification(23) in PLF-AS have also been verified in previous studies.

Although the present study was not designed to demonstrate its prognostic implication, the tendency towards worse functional capacity and also, adverse cardiovascular outcomes in PLF-AS may be due to the subclinical myocardial dysfunction (worse GLS) in this group of patients. Moreover, global strain has been shown to be a significant prognostic factor in patients with heart

failure(4, 24), myocardial infarction(10) and systolic dysfunction(25). Recently, Lancellotti et.al. have demonstrated that strain may be a good index in predicting future outcomes in asymptomatic moderate to severe AS(23). In addition, we could demonstrate that GLS showed a fairly good correlationship with E/E', which is accepted as a reliable echocardiographic parameter with good clinical prognostic value(26). Also, in our analysis of patients who refused or did not undergo surgery, there were significant differences in GLS between those with events and those without, which may imply the prognostic significance of GLS.

Global LV afterload as a determinant of myocardial dysfunction

It is of note that global LV afterload was the significant determinant of myocardial function in severe AS. Of note, all of the diagnostic criteria of severe AS, that is peak transaortic velocity, mean transaortic PG, AVA and valvuloarterial impedance showed multicolinearity, which indicates that all of these factors contribute to the determination of myocardial function. This is also demonstrated by recent works demonstrating that those factors are significant predictors of one year event-free survival and myocardial function (as assessed by midwall shortening) in moderate-severe AS patients(23, 27). These findings have important clinical implication that blood pressure control is important even in severe AS patients, which may contribute to alleviation of increased afterload on the LV.

Study limitations

First, we cannot provide evidence as to whether the improvement of myocardial performance is different in PLF-AS as compared with NF-AS. However, there have been reports suggesting the improvement of strain or strain rate after AVR in AS patients(8, 28) and considering that surgically treated PLF-AS patients carry a similar course as NF-AS patients receiving AVR(2, 3), we can implicate that PLF-AS patients would, at least, show some degree of GLS recovery, leading to a clinical benefit.

Second, the relatively weak correlationship, although statistically significant, shown in our patients may be due to the small sample size. Furthermore, although there was no difference in the aorta dimensions between the two groups, we cannot completely exclude the possibility of bicuspid aortic valve and aortopathy as a possible confounder, especially given the data that there were more bicuspid valve patients in the PLF-AS group.

In conclusion, GLS measured by 2D-STI is depressed in PLF-AS patients. This implies that subclinical myocardial dysfunction is evident in these patients. It also suggests the possible diagnostic value of 2D global strain in PLF-AS. In addition, global LV afterload is an important determinant of myocardial dysfunction in severe AS patients.

CHAPTER 2

Early Detection of Subclinical Ventricular Deterioration with Cardiac Magnetic Resonance in Aortic Stenosis: Two-center Study with Cardiac Magnetic Resonance Imaging and Echocardiography

INTRODUCTION

Aortic stenosis (AS) is a disease that typically provokes pressure overload to the left ventricle, which left uncured, may lead to left ventricular (LV) hypertrophy, pump failure and also, to sudden cardiac death(29, 30). Surgery before the development LV dysfunction is of paramount importance for these patients. Currently, evaluation of symptomatic status and LV ejection fraction (EF) is recommended for determining surgical timing(1). However, sudden cardiac death may occur even in patients without symptom and LV dysfunction. Furthermore, LV diastolic dysfunction(31) and exercise intolerance(18) often persist even after the corrective surgery suggesting the presence of irreversible myocardial damage before surgery. These disappointing results are partly due to poor sensitivity of LVEF as a marker of myocardial damage and thus some investigators support early surgery in asymptomatic patients with normal LVEF(32). Accordingly, early detection of myocardial damage may have clinical impact for these patients.

Before the development of overt pump failure, fibrosis of the LV myocardium ensues(33-35), which leads to diastolic function impairment(36, 37) and possibly occult systolic dysfunction(8, 9, 38). Indeed, patients with severe stenosis of the valve show significant deterioration of the diastolic properties that improves after correction of this stenosis(36, 39). More importantly, the aggravation of diastolic dysfunction is closely related to clinical outcome(40).

Late gadolinium enhancement-cardiovascular magnetic resonance (LGE-

CMR) is the most accurate way to visualize the smallest focal fibrosis/scar in the myocardium(12, 41). Patients with severe AS who had LGE on CMR were more likely to experience worse outcome than those who did not(18, 19, 42, 43). Also, the degree of LGE has also been shown to correlate well with the degree of histological fibrosis in these patients(18). In this report, we investigated whether CMR can be used to detect subclinical deterioration of the ventricular function. Especially, we focused on whether LGE-CMR would discriminate the subtle difference on cardiac function in patients with normal LVEF.

MATERIALS AND METHODS

1. Patient population

A total of 118 patients with moderate to severe AS, i.e. maximal transaortic velocity >3m/sec or mean transaortic pressure gradient >30mmHg and aortic valve area ≤1.5cm^2 were enrolled to this prospective study from September 2009 to September 2012 at both Seoul National University Hospital and Samsung Medical Center, which was composed of a series of echocardiography and LGE-CMR. Patients were consecutively enrolled at the time of echocardiographic examination. Patients with significant concomitant valvular disease of more than mild degree, i.e. moderate aortic regurgitation or moderate mitral valve disease or a previous history of cardiac surgery or myocardial infarction were excluded. All except 9 patients underwent conventional coronary angiography or computed tomography coronary angiography for the presence of significant concomitant coronary artery disease. All patients gave informed consent to the study, the protocol of which was approved by the Institutional Review Board of both institutions. Baseline laboratory tests, anthropometric measures and medical history were taken at the time of echocardiographic examination. Body surface area was calculated with the Mosteller formula.

2. Echocardiographic examination

All patients underwent a comprehensive echocardiographic examination with an adequate commercialized equipment (Vivid 7, GE Medical System,

Horten, Norway) according to the current recommendations(44).

In brief, LV dimensions both at end-diastole and systole were measured at the standard parasternal short-axis view of papillary muscle level or parasternal long-axis view. The dimensions of the aortic root, i.e. aortic annulus, sinotubular junction and ascending thoracic aorta diameter were measured at the standard parasternal long-axis view.

Peak early and late diastolic velocity at the mitral valve tip level (E, A velocity, respectively) and mitral annular velocity (e', a' velocity, respectively) at the septal annulus were measured at the standard apical four-chamber view. Transaortic mean pressure gradient and maximal velocity was measured at all views possible, i.e. apical 5 or 3 chamber, subcostal, right parasternal and suprasternal notch view. Aortic valve area (AVA) was calculated using the continuity equation after acquiring time-velocity integral at the aortic valve level and also, left ventricular outflow tract level. All echocardiographic measurements were averaged for three beats for patients in sinus rhythm and five beats in atrial fibrillation with baseline heart rate of <100BPM.

3. Calculation of LV load and stiffness parameters

The diastolic properties of the LV were estimated using the following parameters. LV filling pressure was estimated by dividing E with e'(45) and to estimate the diastolic elastance of the LV (Ed), E/e' was again divided by the stroke volume measured by CMR(46).

To estimate the systolic stiffness of LV, single beat-derived LV end-systolic elastance (Ees) was calculated as end-systolic pressure/end-systolic volume

(measured by CMR), where end-systolic pressure was calculated as 0.9×(systolic blood pressure).

4. Cardiac magnetic resonance imaging

Cardiac magnetic resonance imaging was performed using a 3.0-T scanner with phased-array receiver coils (Sonata Magnetom, Siemens, Erlangen, Germany) under the standard protocols. In brief, steady-state free precession cine images under an adequate breath-hold were performed to visualize the LV wall motion and also, to quantify the LV function and mass. The entire LV short-axis images were acquired at a 6mm interval from the base to apex to include the whole LV volume. The LGE images were acquired 10 minutes after intravenous gadolinium injection (0.1 mmol/kg Magnevist; Schering, Berlin, Germany). The protocol for the LGE images were as follows; slice thickness 8mm, interslice gap 2mm, TR 9.1msec, TE 42msec, flip angle 13 degrees, in-plane resolution 1.4×1.9mm. Inversion delay time varied from 280~360msec according to the time to null the normal myocardium.

The LGE-CMR images were analyzed by an experienced radiologist blinded to the patients' information. In addition, the region of myocardial fibrosis was defined as the sum of pixels with signal intensity above 5SD of the normal myocardium at each short-axis slice(19), using an appropriate postprocessing program (CMR42, Circle Cardiovascular Imaging Inc., Calgary, Canada). Summation of the measured areas of LGE and the whole myocardium in all short-axis slices yielded the total volume of LGE and the total volume of LV. The percentage of myocardial fibrosis per total

myocardium (%LGE-positive myocardium) was analyzed as the total pixels of fibrosis per total pixels of myocardium.

In addition, the pattern of LGE was classified according to the following classification. The subendocardial LGE pattern was designated if the LGE was located at the subendocardium. All other form of LGE was located along the midwall. If the LGE spanned at least half of a single myocardial segment, it was defined as a linear pattern LGE or otherwise it was defined as a spot pattern LGE. The LGE pattern showing a diffuse fuzzy pattern of enhancement was defined as a patchy pattern LGE. Patients with a mixed pattern of LGE categorized above was classified according to the predominant pattern of LGE.

5. Statistical Analysis

Continuous variables are presented as mean (SD). The difference between two groups was compared using Student's t-test. The difference between three groups was calculated using analysis of variance (ANOVA). Bivariate correlation analysis between the parameters of myocardial function, i.e. diastolic and end-systolic elastance, and the percentage of myocardial fibrosis per total myocardium was drawn. The results of the strength of correlation were presented as Spearman's rho correlation coefficients because of the non-normal distribution of the percentage of myocardial fibrosis per total myocardium. Dichotomous variables are presented as number (percentage) and compared using $\chi 2$-test. All analysis was done with SPSS version 16.0

(SPSS Inc., Chicago, IL) and two-tailed p-value of <0.05 was considered statistically significant.

RESULTS

A total of 118 moderate to severe AS patients were prospectively enrolled for the current study (**Table 2-1**). Approximately half of these patients showed delayed enhancement on LGE-CMR and 15% of the patients had LV systolic dysfunction defined as LVEF<50% on CMR. However, there was no patient with LV systolic dysfunction but without LGE. Therefore, the patients were grouped into three as the following; group 1, no LGE on CMR and normal LV systolic function, group 2, LGE on CMR but normal LV systolic function, and group 3, LGE on CMR and also depressed LV systolic function (**Figure 2-1**).

Baseline clinical characteristics are summarized in Table 2-1. In brief, there were no significant differences in basic anthropometric measures except for the smoking status. All except 5 patients in group 1 and 4 patients in group 2 underwent evaluation for the presence of significant concomitant coronary artery disease but there was no difference between the groups.

The baseline echocardiography parameters are summarized in Table 2-2. Compared with group 1 and 2, the patients in group 3 had significantly larger LV dimensions, longer deceleration time and smaller mitral septal annular velocity. Also as a consequence of LV systolic dysfunction in group 3, the peak transaortic velocity was smaller on Doppler echocardiography. There was also a tendency towards thicker interventricular septum and posterior wall thickness in group 2 compared with group 1. On CMR, there were significant differences in all parameters, including LV volume, LV systolic function and output and also, LV mass (**Table 2-3**) between group 1, 2 and 3.

	Total (n=118)	Group 1 (n=54)	Group 2 (n=45)	Group 3 (n=19)	p-value
Age (years)	68 (10)	68 (10)	68 (10)	69 (11)	0.929
Male, n (%)	34 (50.0)	23 (56.1)	11 (40.7)	11 (40.7)	0.215
SBP (mmHg)	125 (18)	128 (18)	125 (16)	118 (20)	0.108
DBP (mmHg)	69 (11)	70 (12)	69 (12)	66 (9)	0.349
BSA (m^2)	1.65 (0.17)	1.65 (0.16)	1.67 (0.18)	1.63 (0.17)	0.681
Baseline Cr (mg/dL)	0.93 (0.23)	0.92 (0.25)	0.92 (0.20)	0.95 (0.22)	0.877
Hypertension, n (%)	68 (57.6)	33 (61.1)	25 (55.6)	10 (52.6)	0.763
Diabetes, n (%)	29 (24.6)	10 (18.5)	13 (28.9)	6 (31.6)	0.364
Hyperlipidemia, n (%)	25 (21.2)	17 (31.5)	6 (13.3)	2 (10.5)	0.410
Current smoker, n (%)	22 (18.6)	6 (11.1)	8 (17.8)	8 (42.1)	0.011
Af, n (%)	10 (8.5)	5 (9.3)	2 (4.4)	3 (15.8)	0.317
Coronary artery disease, n (%)[§]	16 (14.7)	8 (16.3)	5 (12.2)	3 (15.8)	0.849

Table 2-1. Baseline clinical characteristics of the study participants

All patients were grouped according to the presence/absence of late gadolinium enhancement (LGE) and left ventricular (LV) systolic dysfunction, defined as LV ejection fraction (EF)<50%. Group 1 was defined as normal LVEF and no LGE on CMR (left upper quadrant), group 2 as normal LVEF with LGE on CMR (right upper quadrant), group 3 as depressed LVEF with LGE on CMR (right lower quadrant). The difference of baseline clinical characteristics between the groups was calculated using Student's t-test and the results presented as p-value. NYHA, New York Heart Association. The

data are presented as mean (SD) or number (percentage). SBP/DBP, systolic/diastolic blood pressure; BSA, body surface area; Cr, creatinine; Af, atrial fibrillation. [§]The evaluation of the presence/absence of coronary artery disease was evaluated in 109 patients.

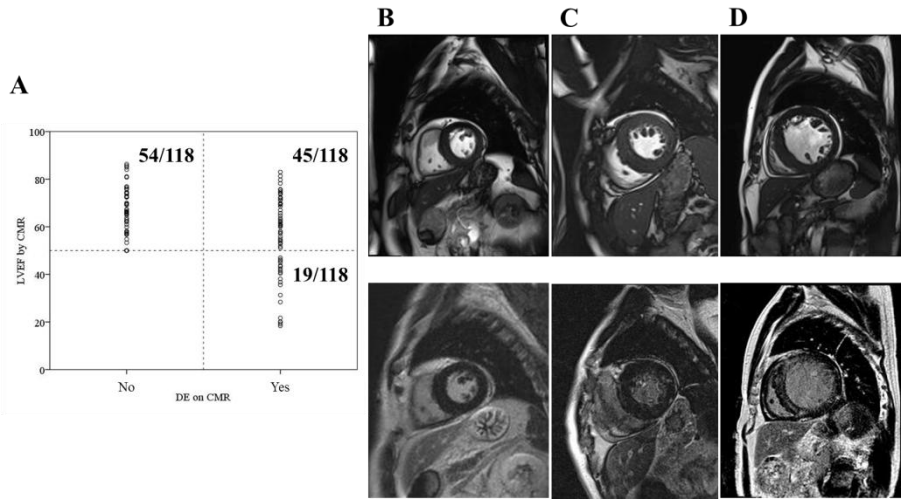

Figure 2-1. Grouping of the study population and representative LGE-CMR images of patients with and without delayed enhancement.

(A) All patients were grouped according to the presence/absence of late gadolinium enhancement (LGE) and left ventricular (LV) systolic dysfunction, defined as LV ejection fraction (EF)<50%. Group 1 was defined as normal LVEF and no LGE on CMR (left upper quadrant), group 2 as normal LVEF with LGE on CMR (right upper quadrant), group 3 as depressed LVEF with LGE on CMR (right lower quadrant). (B) Representative cine and LGE-CMR images of a patient in group 1. (C) Representative cine and LGE-CMR images of a patient in group 2. (D) Representative cine and LGE-CMR images of a patient in group 3.

	Total (n=118)	Group 1 (n=54)	Group 2 (n=45)	Group 3 (n=19)	p-value
LVEDD (mm)	51 (5)	49 (5)	50 (5)	59 (7)‡	<0.001
LVESD (mm)	33 (8)	30 (4)	31 (4)	46 (9)‡	<0.001
IVST (mm)	12 (5)	11 (2)	13 (6)*	13 (6)	0.080
PWT (mm)	11 (2)	10 (2)	11 (2)*	11 (2)	0.036
Annulus diameter (mm)	21 (2)	21 (2)	21 (3)	22 (3)	0.902
E (m/sec)	0.77 (0.28)	0.73 (0.23)	0.79 (0.28)	0.83 (0.40)	0.386
DT (m/sec)	252 (78)	246 (71)	270 (81)	226 (85)†	0.088
e' (cm/sec)	4.8 (1.6)	5.3 (1.7)	4.7 (1.3)	3.9 (1.6)†	0.005
Vmax (m/sec)	4.7 (0.8)	4.6 (0.8)	4.9 (0.8)*	4.3 (0.7)‡	0.015
AVA (cm^2)	0.76 (0.21)	0.79 (0.20)	0.75 (0.21)	0.70 (0.25)	0.291
AVA index (cm^2/m^2)	0.46 (0.13)	0.48 (0.13)	0.45 (0.12)	0.43 (0.14)	0.234
Transaortic mean PG (mmHg)	54 (22)	52 (21)	59 (19)	50 (28)	0.152

Table 2-2. Echocardiographic parameters of the study participants.

The data are presented as mean (SD). LV, left ventricle; EDD/ESD, end-diastolic/systolic diameter; IVST, interventricular septal thickness; PWT, posterior wall thickness; E, early diastolic velocity at mitral valve tip; DT, deceleration time; e', early mitral annular velocity at the septal annulus; Vmax, maximal transaortic velocity; AVA, aortic valve area; PG, pressure gradient.

[*]$p<0.01$ versus group 1, [†]$p<0.01$ versus group 2, [‡]$p<0.05$ versus group 2.

	Total (n=118)	Group 1 (n=54)	Group 2 (n=45)	Group 3 (n=19)	p-value
LVEDV index (mL/m^2)	98.9 (33.5)	84.7 (22.9)	97.3 (25.1)§	143.4 (38.9)‡	<0.001
LVESV index (mL/m^2)	41.0 (30.1)	28.5 (13.2)	35.1 (16.5)*	90.6 (39.3)‡	<0.001
LV ejection fraction (%)	61.4 (15.1)	67.3 (9.8)	65.3 (9.7)	35.2 (10.6)‡	<0.001
LV cardiac index (L/min/m^2)	3.94 (1.07)	3.72 (1.03)	4.35 (1.05)§	3.50 (0.88)‡	0.002
LV mass index (g/m^2)	100.8 (37.4)	86.0 (29.6)	108.0 (40.9)§	125.5 (31.2)	<0.001
DE(+) myocardium/total myocardium (%)	4.18 (5.75)	0	6.91 (5.03)	9.60 (7.16)	<0.001

Table 2-3. Cardiovascular magnetic resonance (CMR) parameters of the study participants.

The data are presented as mean (SD).*p<0.01 versus group 1, §p<0.05 versus group 1,†p<0.01 versus group 2,‡p<0.05 versus group 2. LV, left ventricle; EDV/ESV, end-diastolic/systolic volume; DE, delayed enhancement. §The pattern of LGE was evaluated in 70 patients enrolled at Seoul National University Hospital, 33 patients in group 1, 24 patients in group 2 and 13 patients in group 3.

Although there was no significant difference in the AVA between the 3 groups (**Figure 2-2A**), stepwise differences were noted between the three groups in both end-diastolic and end-systolic volumes resulting in a significant trend towards larger LV in group 3 (**Figure 2-2B**). There was also significant difference in the degree of hypertrophy between the three groups (**Figure 2-2C**). Interestingly, although there was no significant difference in the EF between group 1 and 2 (**Table 2-3**), the volumes and mass in group 1 and 2 were notably different, suggesting subclinical adverse LV remodeling in group 2 (**Figure 2-2B and C**).

The pattern of LGE was classified according to the location and the span width of the LGE (**Figure 2-3**). Although the proportion of patients with subendocardial LGE pattern (**Figure 2-3A**) was similar in group 2 and 3 (14/45 (31.1%) in group 2 vs. 6/19 (31.6%) in group 3), the proportion of patients with spotty pattern (**Figure 2-3B**) was lower in group 3 than group 2 (21/45 (46.7%) in group 2 vs. 4/19 (21.1%) in group 3). On the contrary, the linear LGE pattern (**Figure 2-3C**) was more frequent in group 3 (4/45 (8.9%) in group 2 vs. 7/19 (36.8%) in group 3). The proportion of patients with patchy pattern (**Figure 2-3D**) were similar between the two groups (6/45 (13.3%) in group 2 vs. 2/19 (10.5%) in group 3). Altogether, the pattern of LGE was different between the two groups (p-value=0.038).

Next, we analyzed whether there was any difference between the three groups in the functional remodeling parameters of the LV, i.e. diastolic and systolic function. Left ventricular filling pressure, as estimated by E/e' and diastolic elastance, Ed was compared. There was a significant trend towards

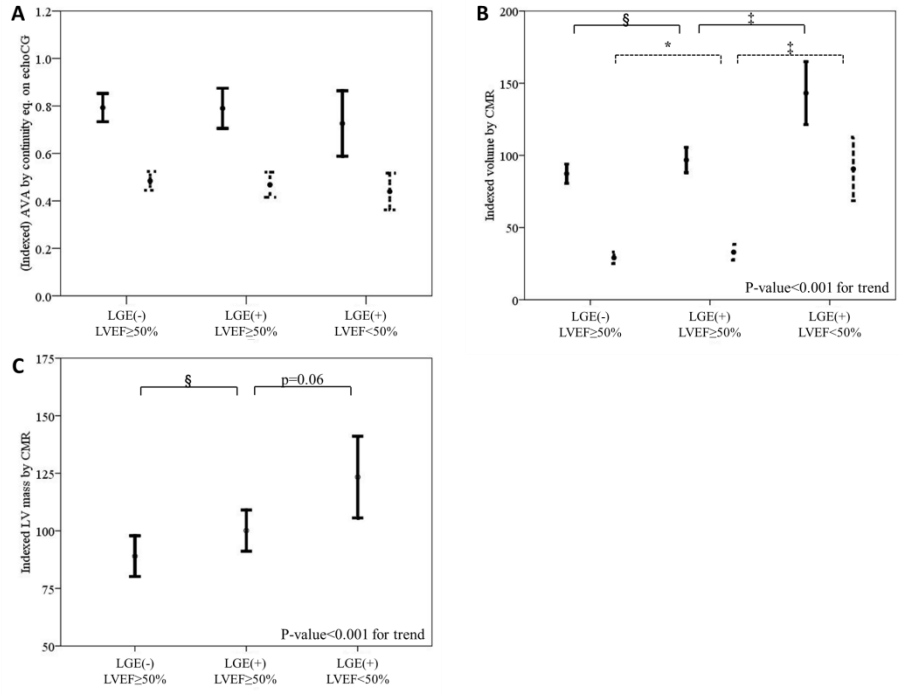

Figure 2-2. Structural LV remodeling assessed with CMR according to the group.

(A) No significant trend in AVA (solid line) nor indexed AVA (dotted line) according to the group of patients. (B) Significant trend in both indexed LV end-diastolic volume (solid line) and indexed LV end-systolic volume (dotted line) according to the group of patients. P-value for trend <0.001 in both parameters. (C) Significant trend in indexed LV mass according to the group of patients.).*p<0.01 versus LGE(-) & LVEF≥50% group, §p<0.05 versus LGE(-) & LVEF≥50% group, †p<0.01 versus LGE(+) & LVEF≥50% group, ‡p<0.05 versus LGE(+) & LVEF≥50% group.

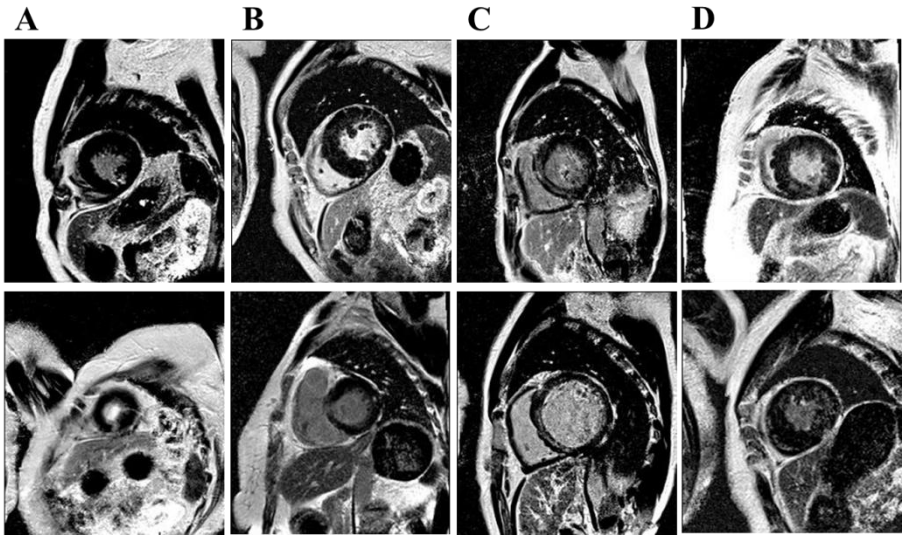

	Subendocardial	Spot	Linear	Patchy	p-value
Group 2 (n=45)	14 (31.1)	21 (46.7)	4 (8.9)	6 (13.3)	0.038
Group 3 (n=19)	6 (31.6)	4 (21.1)	7 (36.8)	2 (10.5)	

Figure 2-3. Diverse pattern of LGE in the study population.

(A) A subendocardial pattern of LGE. (Top panel) A focal subendocardial LGE at the inferior segment. (Bottom panel) Two small subendocardial LGE's at the apicoinferior and apicolateral segments. (B) A spot pattern LGE. (Top panel) Two focal spot LGE's located at the posterior RV attachment site to the septum and also at the inferolateral segment at the subepicardium. (Bottom panel) A tiny spot LGE at the basal anterolateral segment. (C) A linear pattern LGE, spanning at least half of a myocardial segment. Two examples of linear pattern LGE located at the septum. (D) A patchy pattern LGE. (Top panel) Patchy type LGE located from the inferoseptum to the inferolateral segments. (Bottom panel) Patchy LGE located at from the anteroseptum to the

inferolateral segments. p-value=0.038 for χ^2-test.

worse diastolic function as shown by the gradual increase of E/e' and Ed by the groups (**Figure 2-4A and B, Table 2-4**). In terms of end-systolic stiffness, there was also a significant trend towards decreasing end-systolic elastance and also, significant difference in the end-systolic elastance between the 3 groups (**Figure 2-4C, Table 2-4**). It was also notable that the stiffness parameters, Ed and Ees, in group 1 and 2 were different, which suggested advanced LV functional impairment in group 2 (**Figure 2-2B and C, Table 2-4**). There was also a significant trend towards worse functional capacity (**Figure 2-5**).

To dissect the association of the degree of myocardial fibrosis with LV functional remodeling, correlation between the % fibrosis and diastolic stiffness parameter, Ed or systolic stiffness parameter, Ees was drawn. There was a significant positive correlation between Ed and % LGE-positive myocardium (**Figure 2-6A**, Spearman's ρ=0.256, p=0.005), in contrast to a significant negative correlation between Ees and % LGE-positive myocardium (**Figure 2-6B**, Spearman's ρ=-0.359, p<0.001). In addition, there was a significant positive correlation between E/e' and % LGE-positive myocardium (Spearman's ρ=0.233, p=0.012) and between e' and % LGE-positive myocardium (Spearman's ρ=-0.248, p=0.007). Also, there was a significant positive correlation between LV mass index by CMR and % LGE-positive myocardium (**Figure 2-6C**, Spearman's ρ=0.319, p<0.001). The correlation between % LGE-positive myocardium and the AS severity was nonsignificant (Spearman's ρ=-0.139, p=0.134 for indexed AVA; Spearman's ρ=-0.042, p=0.650 for transaortic mean pressure gradient; Spearman's

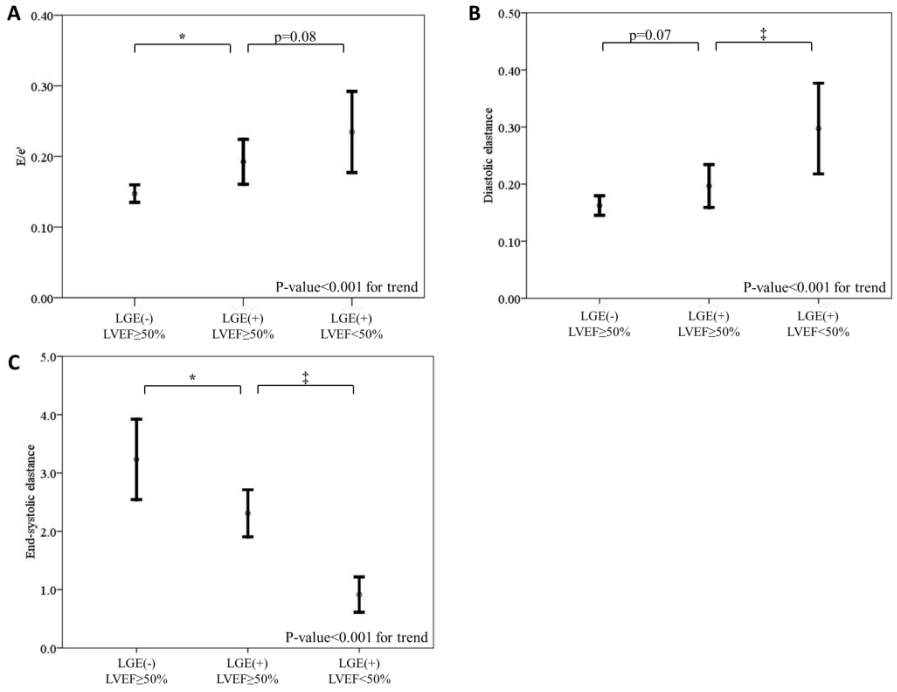

Figure 2-4. Functional LV remodeling assessed with CMR according to the group.

(A) Significant trend in E/e', a parameter of LV filling pressure, according to the group of patients. P-value for trend <0.001. (B) Significant trend in diastolic elastance (Ed), a parameter of diastolic LV chamber stiffness, according to the group of patients. P-value for trend <0.001. (C) Significant trend in end-systolic elastance, a parameter of systolic LV chamber stiffness, according to the group of patients. P-value for trend <0.001.).* $p<0.01$ versus LGE(-) & LVEF≥50% group, ‡ $p<0.05$ versus LGE(+) & LVEF≥50% group. See Figure 1 and 2 for other symbols or abbreviations.

	Total (n=118)	Group 1 (n=54)	Group 2 (n=45)	Group 3 (n=19)	p-value
E/e'	17.3 (8.3)	14.6 (4.3)	18.2 (9.4)*	22.9 (10.8)	<0.001
Ed (mL-1)	0.20 (0.12)	0.17 (0.06)	0.20 (0.12)	0.31 (0.16)‡	<0.001
Ees (mmHg/mL)	2.54 (1.91)	3.24 (2.31)	2.38 (1.16)*	0.93 (0.56)‡	<0.001

Table 2-4. Left ventricular (LV) chamber stiffness parameters of the study participants

The data are presented as mean (SD). *p<0.01 versus LGE(-) & LVEF≥50% group (group 1), ‡p<0.05 versus LGE(+) & LVEF≥50% group (group 2).

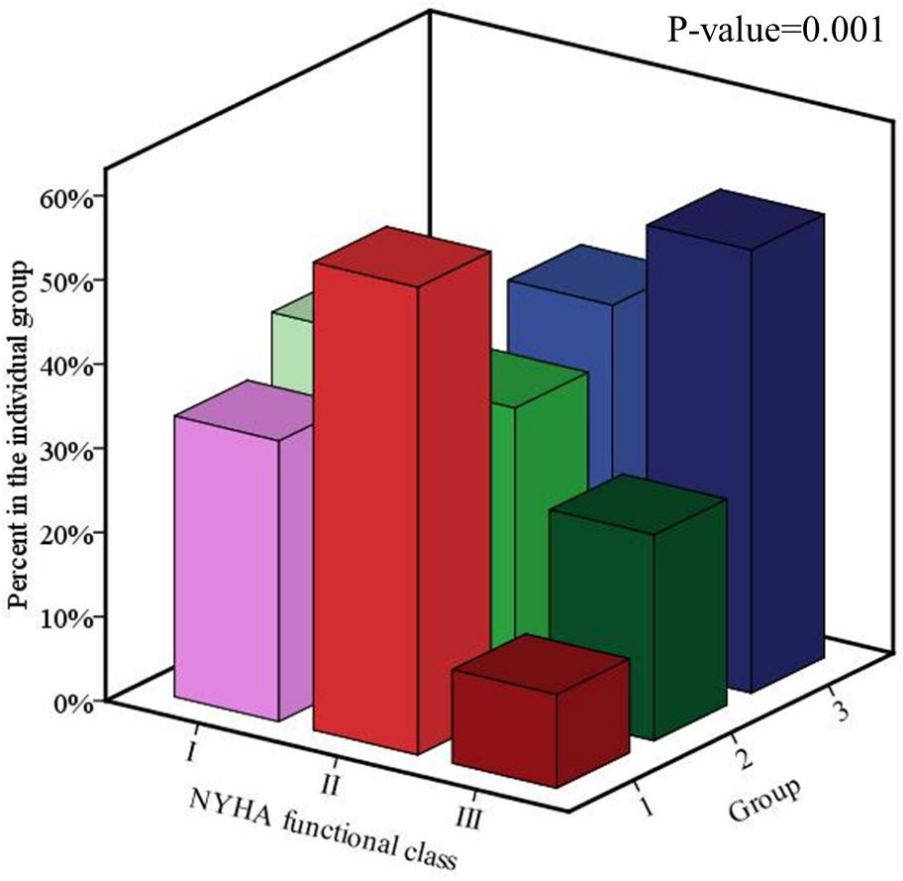

Figure 2-5. Functional status of the patient according to the group.

The functional status of each patient was graded according to the New York Heart Association (NYHA) classification. A significant trend was found in NYHA functional class according to the group of patients. See Figure 2-1 and 2-2 for other symbols or abbreviations. Group 1, LVEF≥50% and no DE on CMR; group 2, LVEF≥50% with DE on CMR ; group 3, LVEF<50% with DE on CMR.

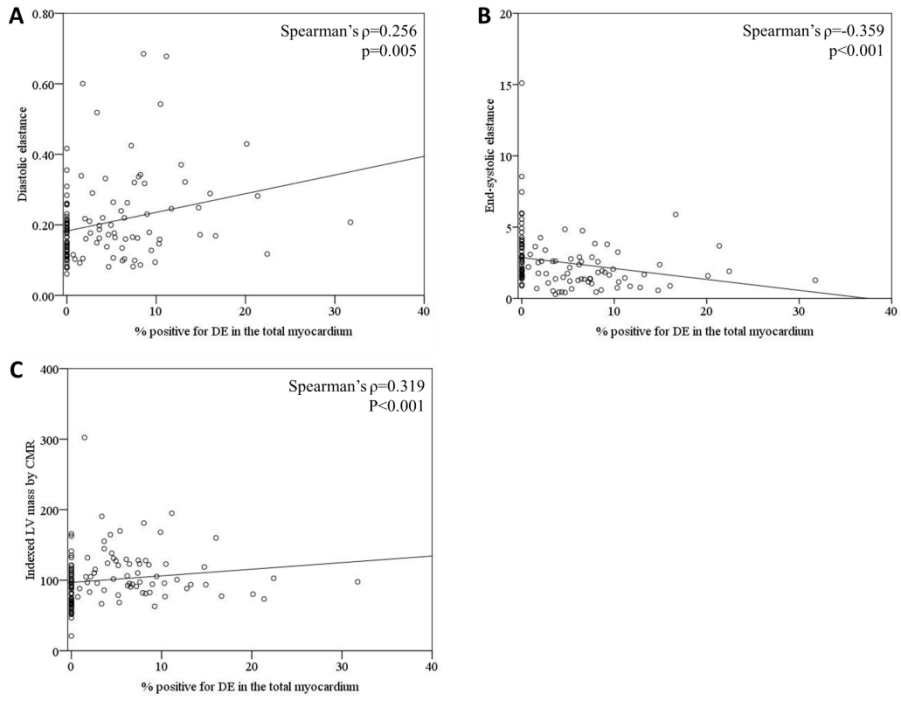

Figure 2-6. Correlation of LV functional parameters and LV mass with the degree of myocardial fibrosis.

LGE was considered present when the signal intensity of the index myocardial segment was greater than 5SD of the remote normal myocardial signal. Significant (A) positive correlation between the degree of LGE and diastolic LV chamber stiffness (diastolic elastance, Ed), (B) negative correlation between the degree of LGE and systolic LV chamber stiffness (end-systolic elastance, Ees) and (C) positive correlation between the degree of LGE and indexed LV mass.

ρ=0.089, p=0.340 for peak transaortic velocity).

DISCUSSION

By dividing the study population into 3 groups according to the presence/absence of LGE and LV systolic dysfunction on CMR, parameters predictive of outcome in severe AS patients(18, 19, 42, 43, 47), we could show that there is a significant trend towards adverse structural and functional remodeling in severe AS patients if there is LGE and LV systolic dysfunction on CMR. More importantly, even if the LVEF was normal, those with LGE on CMR had significantly stiffer LV compared with those without, which suggest that LGE-CMR may be useful for early detection of subclinical LV structural and functional deterioration in severe AS patients with normal LVEF.

Basic Pathophysiologic Mechanism underlying the LV response to AS

The LV loaded with chronic pressure undergoes hypertrophy according to the Laplace's law, which is also accompanied by elevation of end-diastolic pressure(48). Following this, the myocardial perfusion pressure falls(49) and subsequently, myocardial ischemia ensues. The eventual endpoint of this cascade is cardiomyocyte apoptosis, myocardial fibrosis replacing the apoptotic myocytes(33) and subsequently, gradual deterioration of the LV systolic function. In our cohort of patients, none of the patients had LV systolic dysfunction but no LGE. In other words, all patients with LV systolic dysfunction had some degree of LGE in the myocardium. These findings support a general cascade of 'Aortic valve stenosis → LV hypertrophy → Myocardial fibrosis → Ventricular stiffness'.

Previous studies in AS patients have demonstrated that the degree of myocyte apoptosis and myocardial fibrosis correlates well with the degree of LV systolic function deterioration(33). Also, the degree of myocardial fibrosis detected by endomyocardial biopsy tended to show a significant trend to myocyte hypertrophy and LV dilatation(18). These findings verify that the above concepts are indeed the situation that occurs in the setting of AS.

Analysis of our cohort demonstrated a significant trend towards increase of LV volume, mass and LV systolic/diastolic stiffness according to the presence of LGE and LVEF depression, which is in line with the above concepts and findings. This trend in our paper provides a proof-of-concept about the structural pathophysiologic response in AS and how myocardial fibrosis is related to the LV remodeling process.

Myocardial Function in Severe AS and its Relationship with LGE

Several previous papers have demonstrated that LVEF may not be an optimal parameter for reflecting the true myocardial function in severe AS(2, 50). More specifically, there are a substantial proportion of patients with normal EF that display significant depression of myocardial contractility(38) and subsequently a worse prognosis(2, 3). In this aspect, our paper provides direct evidence that even focal myocardial scar demonstrated on CMR may be related to ventricular stiffness in both diastolic and systolic phase, which is in line with a previous paper demonstrating a similar finding(18). As discussed above, the demonstration of focal scar may be a marker of the degree of

cardiomyocyte apoptosis, which in turn may turn out to be deterioration of the systolic and diastolic ventricular function.

It has been suggested that the midwall mechanics of LV may be the determinant of myocardial contractility in AS(51). Although the patterns of LGE are diverse in patients with AS, it was interesting to see a significant proportion of patients with midwall fibrosis(43) in our cohort. Moreover, patients with overt LV systolic dysfunction (LVEF<50%) were more likely to demonstrate a linear pattern of LGE in the midwall, suggesting an important role of midwall contractility. Importantly, a recent paper has nicely shown that the midwall LGE carries a similar risk of mortality as the infarct pattern LGE(43), which could be explained by the depression of the myocardial contractility.

Evidence of Diverse LV Response Patterns in Severe AS

Although the general concept of 'Aortic valve stenosis → LV hypertrophy → Myocardial fibrosis → Ventricular stiffness' has been previously shown in previous papers(48) and our analysis as well, the results of our paper also demonstrated that the correlation between each step was not robust. For example, there was no significant correlation between the degree of aortic valve area and myocardial fibrosis, which suggest that aortic stenosis *per se* may be only one of the contributing factors accelerating myocardial fibrosis.

Although only a few papers have addressed this question directly, factors such as age(18), diabetes(37) and genetic polymorphism(52) have all been suggested as 'contributors' of myocardial fibrosis. The pace of AVA change

may also affect the degree of LVH. Furthermore, previous study has also demonstrated that the correlation between AVA and the degree of LVH may be poor(53). These suggest that the process directing 'Aortic valve stenosis → Myocardial fibrosis' is a multifactorial process involving various factors in between and that the severity of AS should also take into account the ventricular response to pressure overload rather than the numerics associated with the valve itself(23). Also, in this context, parameters to directly assess diffuse myocardial fibrosis such as postcontrast T1 values(54) or T1 mapping with various CMR sequences(55) and its correlation with ventricular function are awaited in the future.

Utility of CMR in Detection of Subclinical Myocardial Dysfunction

One of the most interesting and novel finding in this paper is that even in patients with normal systolic function, patients with LGE tend to have stiffer LV chamber, elevated E/e' and Ed and lower Ees. These findings tell us that even in patients with normal systolic function, a process of subclinical LV dysfunction ensues in patients with LGE on CMR. Although there have been reports demonstrating the prognostic value of LGE on CMR in patients with AS(18, 19, 43), the guidelines dealing with the timing of intervention uses only LVEF as the criteria. As suggested in a recent review of adjunct criteria for assessment of AS(50), our data suggests that the result of LGE-CMR may be integrated as an adjunct criteria for surgical intervention in these group of patients.

Limitations of the Study

Our paper is not without limitations. First, the size of the population was not large. However, the accurate assessment of LV volume, function and mass by CMR demonstrated that, in spite of the small sample size, there was a significant difference in these parameters between patients with versus without LGE. Moreover, our cohort is one of the largest reports so far in terms of AS assessed with CMR. Furthermore, out cohort is the largest one to combine two imaging modalities simultaneously for assessing the remodeling of LV in AS patients. Second, we cannot provide a definite clinical implication as to whether the stiffness parameters are predictors of outcome in these patients. However, there was a significant trend toward worse functional capacity in patients with LGE and LV systolic dysfunction, which suggests that patients with LGE may do worse than those without as in previous papers(18, 42, 43). We do think that more data is desperately needed on the functional outcome in the future. Third, the degree of LGE was not matched with the histological findings. However, it has been persistently proved by previous papers that the degree of LGE shows robust correlation with the degree of histological fibrosis(18, 19).

In conclusion, our analysis results demonstrate that with the use of CMR, it may be possible to detect subclinical LV structural and functional deterioration in severe AS patients. The efficacy of studying LV remodeling comprehensively in predicting the ventricular structural and functional remodeling in severe AS patients warrants further in-depth investigation.

CHAPTER 3

Association of Myocardial Angiogenesis with Structural and Functional Ventricular Remodeling in Severe Aortic Stenosis Patients with Normal Ejection Fraction

INTRODUCTION

Aortic stenosis (AS) is a prototypical disease of pressure overload to the left ventricle, which affects 2~4% of the elderly population(56). It is a gradual but constantly progressive disease with a prolonged asymptomatic period. However the prognosis is poor when symptoms develop(57) and the only curative measure is replacement of the diseased valve at the right time. Therefore, understanding the mechanism of left ventricular (LV) response to pressure overload in these patients is important not only for the optimal timing of surgery but also, for predicting the outcome and possibly, excavating new therapeutic targets.

With a prolonged period of pressure overload, hypertrophy of the myocardium develops as a compensatory mechanism(50). Microscopically, this is associated with increase of myofiber size and interstitial fibrosis in various human(33, 58) and animal models of ventricular hypertrophy(59). More importantly, the degree of hypertrophy in asymptomatic AS patients has been associated with clinical outcome in numerous previous reports(60, 61) and although commonly regarded as ‘normal’ systolic function, some patients do have subclinical LV systolic dysfunction(38, 50). These results suggest that investigating the mechanism of ventricular hypertrophy may be important for understanding the process of ventricular remodeling in AS patients. However the microscopic change in the process of ventricular hypertrophy, especially before the LV systolic dysfunction starts, is largely unknown in humans.

Angiogenesis is a dynamic process that goes side-by-side with the growth

and regression of an organ. Specifically, angiogenesis has been shown to be associated with ventricular hypertrophy in various animal models(62) and several investigators have tried to harness angiogenesis for treating cardiac hypertrophy(63, 64). Although the disruption of coordinated ventricular hypertrophy and myocardial angiogenesis has been shown to contribute to LV systolic dysfunction in animal models(59) and also in humans(33), the process that underlies the very step of transition to heart failure in humans has not been investigated in depth. Also, the phenomenon that has been demonstrated in animals has to be correlated with various parameters of ventricular function in humans, in order to be translated into clinical research in the future.

Aortic stenosis is an excellent human model for studying the change of ventricular function and morphology following chronic pressure overload(48). In this report, we analyze for the first time the degree of myocardial angiogenesis with various ventricular remodeling parameters in both function and structure.

MATERIALS AND METHODS

1. Patient population

A total of 38 patients with moderate to severe AS as per current guidelines(65) were enrolled to this prospective study from September 2009 to September 2012 at Seoul National University Hospital. Patients with significant concomitant valvular disease of more than mild degree, i.e. moderate aortic regurgitation or moderate mitral valve disease, a previous history of cardiac surgery or myocardial infarction and also, patients with significant LV systolic dysfunction (LVEF<50%) were excluded. All patients gave informed consent to the study, the protocol of which was approved by the Institutional Review Board of Seoul National University Hospital. Baseline laboratory tests, anthropometric measures and medical history were taken at the time of echocardiographic examination. Body surface area (BSA) was calculated using the Mosteller formula.

2. Echocardiographic examination

We performed a comprehensive echocardiographic examination of each patient with an adequate commercialized equipment (Vivid 7, GE Medical System, Horten, Norway) according to the current recommendations and guidelines(44).

In brief, end-diastolic/systolic LV diameter were measured at the standard parasternal short-axis view of papillary muscle level. The ejection fraction (EF) of the LV was calculated using the above diameters of LV. The aortic

root, i.e. aortic annulus, sinotubular junction and ascending thoracic aorta diameter were measured at the standard parasternal long-axis view.

After securing an adequate standard four-chamber view, we measured peak early and late diastolic velocity (E, A velocity, respectively) at the tip of mitral valve using a standard pulsed-wave Doppler and also, mitral annular velocity (E', A' velocity, respectively) at the septal annulus using tissue Doppler imaging. We also measured transaortic mean pressure gradient (PG) and maximal velocity at all possible views, for example apical 5 or 3 chamber, subcostal, right parasternal and suprasternal notch view. Aortic valve area (AVA) was calculated using the continuity equation after acquiring time-velocity integral (TVI) at the aortic valve level and also, left ventricular outflow tract (LVOT) level. Stroke volume was calculated by multiplying TVI at the LVOT level with the cross-sectional area of LVOT and indexed by dividing it with BSA. Valvuloarterial impedance, a measure of the global LV afterload, was calculated using the following equation; (systolic blood pressure + mean transaortic PG) / indexed stroke volume(2). The LV mass was calculated using the equation of Devereux et al(6).

For patients in sinus rhythm, all measurements were an average of 3 consecutive beats. For patients in atrial fibrillation with a baseline heart rate <100BPM, all measurements were an average of 5 beats according to the current recommendations.

The pattern of ventricular remodeling was classified according to the previous literatures using LV mass index and relative wall thickness (RWT), into concentric remodeling, eccentric hypertrophy or concentric

hypertrophy(66).

3. Endomyocardial biopsy

All patients gave written consent on the intraoperative biopsy. In brief, after a standard aortotomy and removal of the diseased aortic valve, 2~3 3mm sized endomyocardial biopsy specimen was collected from the basal septum of the left ventricular cavity using a standard bioptome. The samples were immediately transferred to the laboratory for processing.

4. Immunostaining and morphometric analysis

One tissue sample from one myocardial biopsy specimen was taken. All samples were stored overnight in 10% formaldehyde solution and embedded in paraffin. 4μm section was cut for immunohistochemistry and treated for antigen activation. Nonspecific binding sites were pre-blocked using 3% hydrogen peroxide for 15 minutes. The primary antibody used for detection of blood vessel was rabbit anti-human platelet endothelial cell adhesion molecule-1 (PECAM-1, 1:250, Millipore). The primary antibody was incubated overnight at 4℃ and a secondary biotinylated anti-rabbit IgG (1:100, Promega) antibody was incubated following the primary incubation. Finally, the staining results were visualized using a standard DAB kit (Vector lab.) according to the manufacturer's recommendation. Morphometric measurements and analysis were done with a semi-automatic dedicated software (ImageJ, http://rsb.info.nih.gov/ij). The result of the morphometry was expressed as the PECAM-1 positive % area of the whole image.

5. Statistical Analysis

Continuous variables are tested for normality with Kolmogorov-Smirnov test and presented as mean (standard deviation), median (25^{th} IQR-75^{th} IQR) or number (percentage) as appropriate. The difference between the two groups was compared using Student's t-test or Mann-Whitney U test and analysis of variance (ANOVA) between three groups. Bivariate correlation analysis between the parameters of myocardial structure and function are drawn and the strength of correlation presented as Pearson's correlation coefficients. Dichotomous variables are presented as percentages and compared using $\chi 2$-test. Variables that were considered related to myocardial blood vessel density were initially analyzed with univariable analysis and then, variables with a p-value<0.1 were incorporated into the linear regression model to identify significant factors associated with myocardial blood vessel density. All analysis was done with SPSS version 16.0 (SPSS Inc., Chicago, IL) and two-tailed p-value of <0.05 was considered statistically significant.

RESULTS

A total of 38 severe AS patients were prospectively enrolled for the current study. The baseline clinical characteristics are summarized in Table 3-1 and the baseline echocardiography parameters in Table 3-2. We included only those with normal systolic function, i.e. LV ejection fraction >50%, to analyze how angiogenesis was specifically related to the process just before the transition to heart failure.

Next, we analyzed the blood vessel density in the myocardium that was taken at the time of AVR. There was a wide range of vessel density that ranged from 1% to nearly 4% of the whole section. Various echocardiography parameters including parameters of systolic and diastolic function, i.e. LV ejection fraction, E/e', the degree of aortic valve stenosis, i.e. mean transaortic pressure gradient, maximal transaortic velocity, indexed aortic valve area and also, the degree of LV hypertrophy was analyzed for correlation with the blood vessel density. Of the several parameters, various parameters of ventricular function, such as, LV ejection fraction (**Figure 3-1A**, r=-0.378, p-value=0.019) and E/e' (**Figure 3-1B**, r=0.391, p-value=0.018) showed significant correlation with the blood vessel density. Also, calculated LV mass index (**Figure 3-2A**, r=0.447, p-value=0.005) significantly correlated with myocardial blood vessel density. Although transaortic mean PG and peak velocity did not show significant correlation with the myocardial vessel density, AVA also showed good correlation with the vessel density (**Figure 3-2B**, r=-0.365, p=0.024). These findings demonstrate that the blood vessels

	Total (n=38)	Concentric Remodeling (n=5)	Eccentric Hypertrophy (n=13)	Concentric Hypertrophy (n=20)	p-value
Age (years)	67.7 (8.9)	73.6 (10.8)	64.8 (10.1)	68.2 (7.5)	0.162
Male, n (%)	17 (44.7)	2 (40.0)	7 (53.8)	8 (40.0)	0.718
SBP (mmHg)	126 (16)	132 (14)	128 (19)	124 (14)	0.656
DBP (mmHg)	69 (10)	69 (7)	69 (10)	69 (10)	0.967
Body surface area (m^2)	1.69 (0.14)	1.69 (0.16)	1.73 (0.13)	1.66 (0.14)	0.365
Hypertension, n (%)	17 (44.7)	2 (40.0)	7 (53.8)	8 (40.0)	0.718
Diabetes mellitus, n (%)	11 (28.9)	1 (20.0)	3 (23.1)	7 (35.0)	0.681
Hyperlipidemia, n (%)	6 (15.8)	1 (20.0)	2 (15.4)	3 (15.0)	0.962

Table 3-1. Baseline clinical characteristics of the study participants

The difference of baseline clinical characteristics between patients with distinct patterns of remodeling, i.e. concentric remodeling, eccentric hypertrophy, concentric hypertrophy was calculated using Student's t-test, Mann-Whitney U test or $\chi 2$-test as appropriate and the results presented as p-value. SBP/DBP, systolic/diastolic blood pressure; BSA, body surface area.

	Total (n=38)	Concentric Remodeling (n=5)	Eccentric Hypertrophy (n=13)	Concentric Hypertrophy (n=20)	p-value
LVEDD (mm)	50.5 (5.2)	49.8 (2.2)	53.5 (4.8)	48.5 (4.9)	0.014
LVESD (mm)	31.3 (5.1)	31.0 (1.6)	33.7 (3.5)	29.6 (5.9)	0.067
LVEF (%)	61.7 (6.7)	60.8 (5.7)	60.6 (3.8)	62.7 (8.4)	0.650
IVST (mm)	12.1 (2.4)	10.3 (1.3)	10.6 (1.3)	13.4 (2.3)	<0.001
PWT (mm)	11.6 (1.9)	8.8 (0.5)	10.8 (1.1)	12.7 (1.7)	<0.001
Annulus diameter (mm)	20.8 (1.9)	21.5 (1.9)	21.8 (1.8)	20.1 (1.7)	0.029
E (m/sec)	0.73 (0.19)	0.59 (0.23)	0.73 (0.23)	0.75 (0.15)	0.304
DT (m/sec)	254 (66)	264 (37)	239 (66)	262 (71)	0.577
e' (cm/sec)	4.7 (1.4)	4.9 (2.2)	5.0 (1.3)	4.4 (1.3)	0.466
Vmax (m/sec)	4.7 (0.7)	4.1 (0.2)	4.6 (0.7)	4.9 (0.7)	0.080
AVA (cm^2)	0.73 (0.23)	0.97 (0.37)	0.82 (0.17)	0.63 (0.18)	0.003
Transaortic mean PG (mmHg)	55.8 (19.4)	40.5 (1.8)	50.1 (16.6)	62.9 (20.4)	0.036

Table 3-2. Baseline echocardiographic characteristics of the study participants.

The data are presented as mean (SD). LV, left ventricle; EF, ejection fraction; EDD/ESD, end-diastolic/systolic diameter; IVST, interventricular septal thickness; PWT, posterior wall thickness; E, early diastolic velocity at mitral valve tip; DT, deceleration time; e', early mitral annular velocity at the septal annulus; Vmax, maximal transaortic velocity; AVA, aortic valve area; PG, pressure gradient. $^{*}p<0.01$ versus group 1, $^{\dagger}p<0.01$ versus group 2, $^{\ddagger}p<0.05$

versus group 2.

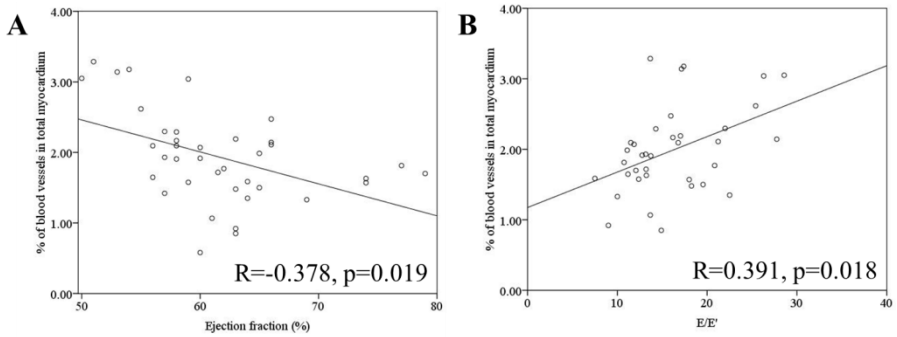

Figure 3-1. Correlation between ventricular function and myocardial blood vessel density.

(A) Significant negative correlation existed between ejection fraction and myocardial blood vessel density, in contrast to (B) significant positive correlation between E/E' and myocardial blood vessel density.

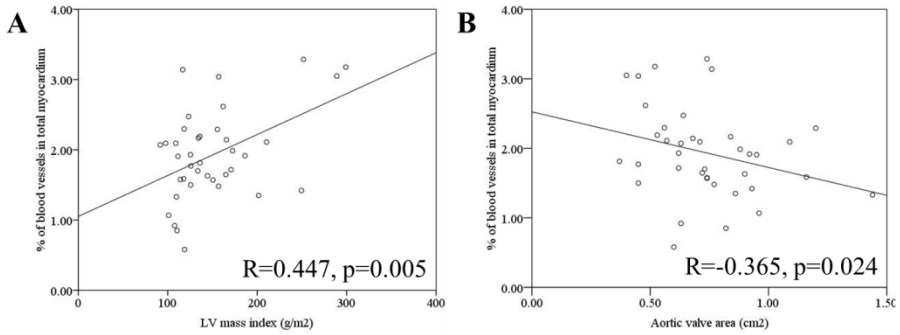

Figure 3-2. Correlation between structural parameters of aortic stenosis and myocardial blood vessel density.

(A) Significant positive correlation existed between left ventricular mass index and myocardial blood vessel density, in contrast to (B) significant positive correlation between aortic valve area and myocardial blood vessel density.

may grow according to the hypertrophy of the LV and also, aggravation of both LV systolic and diastolic function (**Figure 3-3**).

Among the above parameters, linear logistic regression analysis was done to determine the factor responsible for myocardial angiogenesis. Although E/e' and AVA was nonsignificant LV ejection fraction and LV mass index remained as a significant determinant of the degree of angiogenesis (β=-0.313, p=0.028 for LV ejection fraction, β=0.398, p=0.010 for LV mass index). This was not changes even after adding the baseline clinical parameters (β=-0.302, p=0.043 for LV ejection fraction, β=0.377, p=0.033 for LV mass index) (**Table 3-3**).

The patients were subdivided into the LV geometry as in the previous literature(66) and 5 patients with concentric remodeling, 13 patients with eccentric hypertrophy and 20 patients with concentric hypertrophy were analyzed. There was a significant trend towards increasing blood vessel density according to the LV geometry (**Figure 3-4**).

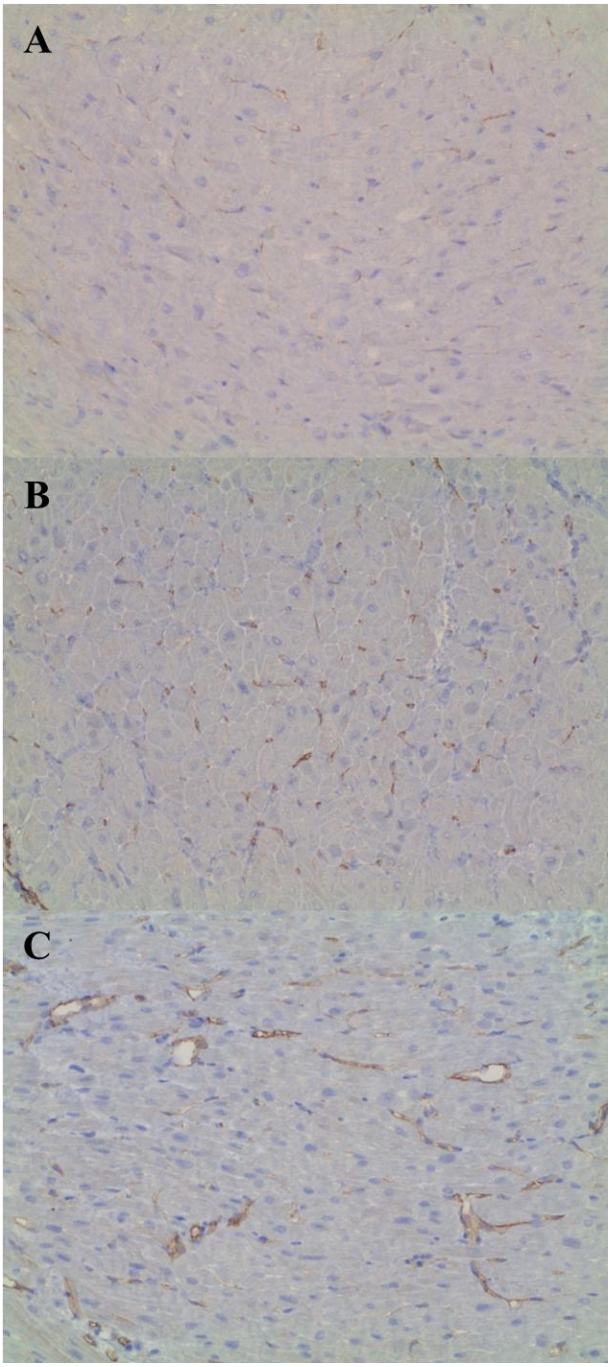

Figure 3-3. Examples of myocardial blood vessels in patients with various remodeling patterns.

(A) A patient with concentric remodeling (LV mass index 112.9g/m^2 and RWT 0.45). The LVEF was 64% and E/E' 7.5. The myocardial blood vessel density was 1.59% of the total myocardium analyzed. (B) A patient with eccentric hypertrophy (LV mass index 134.3g/m^2 and RWT 0.38). The LVEF was 58% and E/E' 16.1. The myocardial blood vessel density was 2.17% of the total myocardium analyzed. (C) A patient with concentric hypertrophy (LV mass index 161.9g/m^2 and RWT 0.49). The LVEF was 55% and E/E' 25.4. The myocardial blood vessel density was 2.62% of the total myocardium analyzed.

	Univariate		Multivariate	
	β	p-value	β	p-value
LV ejection fraction	-0.410	0.011	-0.313	0.028
E/e'	0.441	0.007	0.120	0.459
LV mass index	0.510	0.001	0.398	0.010
AVA	-0.319	0.051	-0.157	0.308
Transaortic mean PG	0.183	0.272		
Transaortic Vmax	0.141	0.397		
Valvuloarterial impedance	0.142	0.402		

Table 3-3. Predictors of myocardial blood vessel density among AS severity parameters.

LV, left ventricle; AVA, aortic valve area; PG, pressure gradient; Vmax, maximal velocity.

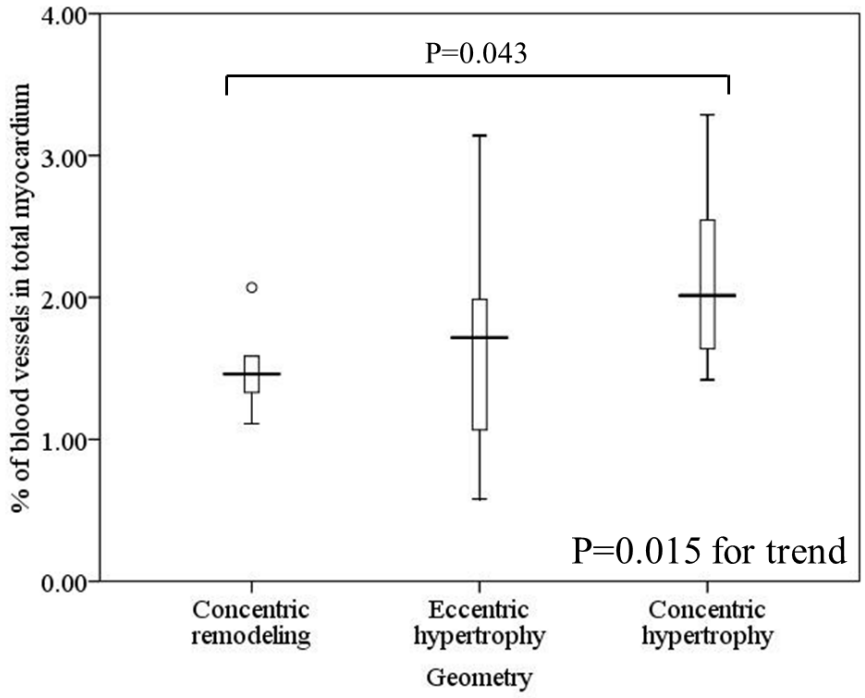

Figure 3-4. Relationship and difference of myocardial blood vessel density according to LV remodeling pattern.

There was a significant trend towards increasing blood vessel density according to worsening LV geometry.

DISCUSSION

The main findings of the current study are that (1) within the similar 'normal' systolic function, a wide degree of myocardial angiogenesis exists in patients with severe AS, (2) the degree of myocardial angiogenesis correlates well with both LV systolic and diastolic function, (3) the degree of myocardial angiogenesis also correlates with the degree of ventricular hypertrophy and AS and finally, (4) there is a trend towards more myocardial angiogenesis with worsening of the LV geometry. Although there have been various animal and human studies with AS investigating the correlation of angiogenesis with overt heart failure(67), there has been no studies showing that angiogenesis is associated with subclinical LV dysfunction in human hearts.

With chronic pressure overload to the left ventricle in AS, the myofibrils tend to get thicker, which results in ventricular hypertrophy(48). This also means that hypertrophy of the ventricles is a dynamic process involving various complex intracellular signals(68, 69). Angiogenesis is a dynamic process that is closely related to organ growth and metabolism of the cells needs ingrowth of blood vessels to support this process(70). Specifically, the disruption of the coordination between ventricular hypertrophy and angiogenesis has shown to be a cause of overt heart failure in murine models(59), which support the previous hypothesis concerning angiogenesis and ventricular hypertrophy. Furthermore, the decreased expression of myocardial vascular endothelial growth factor (VEGF) has been pointed out as the culprit of systolic dysfunction(71, 72).

In this report we have showed that the degree of myocardial angiogenesis is closely associated with adverse remodeling. Specifically, within patients with normal ejection fraction, the systolic/diastolic function, the LV mass and the degree of AS was all closely associated with the degree of myocardial angiogenesis. Following the natural concept that angiogenesis follows the growth of an organ(70) and that the disruption of angiogenic cytokine in the cardiomyocytes leads to systolic dysfunction(71), it can be said that if the systolic function are within normal limits, a certain degree of angiogenesis follows the adverse remodeling of AV with chronic pressure overload. This is supported by some old animal data demonstrating evidence of capillary growth in hypertensive rodent models(73). Furthermore, it is a relatively well-known concept that the coronary vascular resistance/reserve is much reduced with the progression of ventricular hypertrophy, both in animals(74) and in humans(49). Therefore, it may be logical to say that angiogenesis, which inevitably involves the sprouting of new vessels, may be a compensatory mechanism for the decrease of coronary vascular resistance/reserve.

It was interesting to find that the degree of myocardial angiogenesis is not only associated with the degree of adverse LV remodeling but it is fairly ‘well-correlated’ with it. Specifically, the moderate degree of correlation in nearly all of the echocardiographic data tested shows that the process of LV remodeling, although it may be sometimes differ from individual-to-individual, follows a fairly universal process. Following a chronic pressure overload to the LV due to the progression of AS, the ventricular starts to get thicker whilst the systolic and diastolic function deteriorate(48, 50). Although

our data involves only patients with ‘normal’ systolic function, i.e. LV ejection fraction>50%, the results of our analysis demonstrates that the ventricles are undergoing extensive pathological remodeling. Increased angiogenesis may be a compensatory effort of the cardiomyocytes to endure the prolonged stress, which in the long-term may fail(59). Therefore, as previous reports have demonstrated(38), employing more sensitive parameters, such as strain, for assessing the ventricular remodeling may be needed as a guide for effective early treatment(50).

Another interesting finding was that there was a significant trend towards more myocardial angiogenesis in association with the degree of geometric remodeling. This also shows that ejection fraction may not be an accurate method for assessing the systolic function of the LV. Previous data have demonstrated that longitudinal strain, a marker of subendocardial fiber contractility, is decreased in patients with concentric hypertrophy compared with other types of geometry(20). However, neither the circumferential nor the radial strain were affected by the geometry. This finding, in concert with our previous findings(38) and also, the current analysis, demonstrates that the subendocardial layer is the one that undergoes extensive remodeling in response to chronic pressure overload. It is also notable that all of the biopsy specimens used in our analysis were from endomyocardial biopsy taken at the subendocardium.

Our findings are not without limitations. First of all, the hemodynamic data used, especially LV ejection fraction and E/e’, are all load-dependent parameters of LV function. However, all of our patients were in euvolemic

status and did not having resting dyspnea on echocardiographic examination. Second, although we have suggested a possible mechanism for increased angiogenesis following adverse ventricular remodeling in severe AS, we did not prove a definite data for coronary flow reserve nor resistance. Third, a more sensitive and yet a more reliable data for myocardial contractility may serve as a good marker for subclinical myocardial dysfunction, a data that we do not have at the moment. We plan to present these data in the near future.

In conclusion, our analysis results demonstrate that there is a close correlation between the degree of myocardial angiogenesis following adverse remodeling of the LV in severe AS patients with normal ejection fraction. Specifically, myocardial angiogenesis increases as the degree of adverse LV remodeling increases. Further study is warranted on the mechanism of myocardial angiogenesis following chronic pressure overload in humans and how this is related to outcome in the future.

In conclusion, our analysis results demonstrate that there is a close correlation between the degree of myocardial angiogenesis following adverse remodeling of the LV in severe AS patients with normal ejection fraction. Specifically, myocardial angiogenesis increases as the degree of adverse LV remodeling increases. Further study is warranted on the mechanism of myocardial angiogenesis following chronic pressure overload in humans and how this is related to outcome in the future.

CHAPTER 4

Detection of Diffuse Myocardial Fibrosis with Native T1 values on Cardiovascular Magnetic Resonance and its Relationship with Myocardial Function in Asymptomatic Aortic Stenosis Patients

INTRODUCTION

Diffuse myocardial fibrosis is a hallmark of the myocardial response to aortic stenosis (AS)(33, 58). Because of the excessive pressure overload following AS, cardiomyocyte hypertrophy and apoptosis ensues(33) and myofibroblasts are activated, which results in myocardial fibrosis. Furthermore, the degree of myocardial fibrosis is an important prognosticator in severe AS(75). Therefore, there have been numerous efforts to quantify myocardial fibrosis in these patients and also, to analyze the degree of fibrosis with ventricular function.

Cardiovascular magnetic resonance (CMR) was initially applied to accurately image myocardial damage in myocardial infarction patients(41) and among a spectrum of cardiovascular imaging modalities, it has the best spatial resolution for imaging myocardial fibrosis. Specifically, CMR has been applied to AS patients and it has been verified by various investigators that the presence/absence of late gadolinium enhancement (LGE) reflects the prognosis of severe AS patients(18, 19, 43). However, LGE represents focal myocardial fibrosis, which is not reversible after aortic valve replacement (AVR) in severe AS patients(18), whereas diffuse myocardial fibrosis has been reported to be reversible with appropriate treatment(58, 76). Furthermore, following pressure overload, diffuse interstitial fibrosis ensues, preceding focal replacement fibrosis(77, 78). Therefore, proper noninvasive identification of diffuse myocardial fibrosis may be important in predicting the outcome of patients in severe AS, especially in patients undergoing AVR.

In light of this, some investigators have used various techniques other than LGE in CMR to quantify the degree of diffuse myocardial fibrosis(54, 55, 77, 79). However, nearly all of these techniques use gadolinium contrast, which is difficult to use in patients with renal failure(80). In addition, it takes technical expertise to evaluate diffuse myocardial fibrosis using post-contrast T1 value(77). Therefore, a simple and yet, accurate method to evaluate diffuse myocardial fibrosis using CMR is yet to be developed.

In this analysis, we report the clinical utility of native T1 value in evaluating the degree of diffuse myocardial fibrosis in asymptomatic moderate to severe AS patients. We also tested whether the native T1 value in asymptomatic AS patients correlates with subclinical myocardial dysfunction.

MATERIALS AND METHODS

1. Patient population

Asymptomatic patients with moderate to severe AS were enrolled to this prospective cohort study from October 2011 to April 2013 at Seoul National University Hospital. This study was composed of a series of echocardiography and CMR. Moderate to severe AS was defined as the following; maximal transaortic velocity >3m/sec or mean transaortic pressure gradient >30mmHg and aortic valve area $\leq$1.5cm^2(1, 65). Patients with significant concomitant aortic regurgitation of more than moderate degree or significant mitral valve disease of more than moderate degree were excluded. Patients with a previous history of cardiac surgery or myocardial infarction were excluded. Also, symptomatic patients with dyspnea of New York Heart Association III or IV and patients with typical exertional chest pain or syncope were also excluded from the current analysis. The protocol of the study was approved by the Institutional Review Board of Seoul National University Hospital and all patients gave informed consent to the study. Baseline laboratory tests, anthropometric measures and medical history were taken at the time of study enrollment. Body surface area (BSA) was calculated using the Mosteller formula.

2. Echocardiographic examination

Echocardiographic parameters were gathered by an experienced sonographer unaware of the objectives of the current study using an adequate,

commercialized equipment (Vivid 7, GE Medical System, Horten, Norway). All measurements were done following the current guidelines(44, 81).

In brief, end-diastolic/systolic dimensions and thickness of the interventricular septum and posterior wall of the left ventricle (LV) were measured at the standard parasternal short-axis view of M-mode echocardiography. The dimensions of the aortic annulus, sinotubular junction and ascending thoracic aorta diameter were measured at the standard parasternal long-axis view of two-dimensional echocardiography.

Peak early diastolic velocity at the mitral valve tip (E velocity) and mitral annular velocity (e' velocity) at the septal annulus were measured at the standard apical four-chamber view. The mean transaortic pressure gradient and maximal transaortic velocity were measured at all views possible views, i.e. apical 5 or 3 chamber, subcostal, right parasternal and suprasternal notch view. Time-velocity integral at the aortic valve level and the left ventricular outflow tract level was acquired using continuous wave and pulse wave Doppler respectively and aortic valve area (AVA) was calculated using the continuity equation with the above parameters. The AVA was indexed by dividing it with BSA. All echocardiographic measurements were averaged for three beats for patients in sinus rhythm and five beats in atrial fibrillation with baseline heart rate of <100BPM.

3. 2D speckle tracking imaging analysis

A standard 2D-speckle tracking image was taken at a frame rate of 50~100 frame/second after an end-expiratory breath-hold from apical four, three and

two-chamber views and the midventricular short-axis view. The LV endocardial border was carefully traced at the end-systolic phase and the region-of-interest was drawn semi-automatically by an off-line analysis program (EchoPac 5.0.1 for PC, GE Medical System) between the endocardial and epicardial borders. At least five segments were traced properly to get an adequate measurement of global strain. Peak global strain was defined as the peak negative value of the strain curve in a single cardiac cycle and calculated for the entire LV myocardium as follows; global strain=(L[end-systole]–L[end-diastole])/L[end-diastole]×100(%) (L, whole LV myocardium as one big segment)(7). Peak global longitudinal strain (GLS) is an average of GLS values analyzed at apical four, three and two-chamber views. Peak global circumferential strain (GCS) was measured at the midventricular short-axis view. The analysis of 2D-speckle tracking imaging was possible in all patients except for one patient with very poor apical image and for two patients with very poor short-axis image.

4. Cardiac magnetic resonance imaging

We performed CMR using a 3.0-T scanner equipped with adequate phased-array receiver coils (Trio, Siemens, Erlangen, Germany) under the standard protocols. Steady-state free precession cine images were taken under a firm breath-hold to visualize the LV wall motion. All of the entire LV short-axis images were acquired at a 10mm interval from the base to apex to include the whole LV volume and these images were used for analyzing the LV volumes, mass and ejection fraction.

The left atrial (LA) volume was calculated by the following equation based on CMR measurements; LA volume= $8/3\pi\times((A1\times A2)/L)=0.85\times((A1\times A2)/L)$ (A1, LA area on 4 chamber view; A2, LA area on 2 chamber view; L, LA long-axis length determined as the distance of the perpendicular line measured from the middle of the plane of the mitral annulus to the superior aspect of the LA in both the 4- and 2-chamber views. The shortest of these 2 length measurements were used as L.)(44).

All volume and mass measurements were indexed by dividing it with BSA.

After acquiring the cine images, a midventricular short-axis slice at the papillary muscle level and additional basal and apical short axis slices were acquired using the modified Look-Locker inversion recovery (MOLLI) sequence, from three images in the first two Look Locker segments and five images for the third inversion (3-3-5 standard protocol). Finally 11 images over 17 heartbeats were obtained and in-line motion correction and map generation were done(82). The following readout parameters were used; slice thickness 6 mm, TR 2.5 msec, TE 1.1 msec, 6/8 partial Fourier acquisition, field-of-view 300 mm, matrix size 192×125.

The LGE images were acquired 10 minutes after intravenous gadolinium injection (0.1 mmol/kg Magnevist; Schering, Berlin, Germany) using phase sensitive inversion recovery (PSIR) sequence. The protocol for the DE images were as follows; slice thickness 8 mm, interslice gap 2 mm, TR 9.1 msec, TE 4.2 msec, flip angle 20 degrees, in-plane resolution 1.4×1.9 mm. Inversion delay time varied from 280~360msec according to the time to null the normal myocardium.

5. Measurement of native T1

The T1 map images were generated from the MR workstation after in-line motion correction just after image acquisition. The region of interest (ROI) was drawn manually at the midventricular septum according to the previous publication(83, 84), after confirming that there were no definite areas of focal LGE in the ROI. We tried to draw the ROI on the compact myocardium and not to include the border of the myocardium because the border between the myocardium and the LV cavity showed gradual change of T1 value partly from partial volume averaging artifact and partly from registration error even after motion correction. The measurements on T1 map image were performed on the PACS system (Maroview, Infinitt, Seoul, Korea). One radiologist performed all measurements. In randomly selected 14 patients, measurement of T1 value was repeated to check the intraobserver variability and a separate, blinded second observer cross-checked the measurement on the same set of patients to evaluate the interobserver variability.

6. Histological analysis

In a subgroup of patients undergoing AVR for clinical purpose, we gathered 11 biopsy samples from the basal LV septum. In brief, an intraoperative myocardial biopsy of no less than $10mm^3$ was taken and processed for staining with Picrosirius red. Samples with only endocardial biopsy specimens were excluded. The stained samples were visualized using a standard microscopy at high-power magnification (×200). Morphometric

measurements and analysis were done with a semi-automatic dedicated software (ImageJ, http://rsb.info.nih.gov/ij) and the result of the morphometry was expressed as the Picrosirius red-staining positive % area of the whole image.

7. Statistical analysis

Continuous variables are presented as mean (standard deviation) (SD). The distribution pattern was tested for normality using the Shapiro-Wilk test. After dividing the entire population into three groups according to the native T1 value, the difference between these groups was compared using analysis of variance (ANOVA). Bivariate correlation analysis between the various parameters of myocardial function and structure and the native T1 value was drawn. The strength of correlation was presented as Pearson's correlation coefficients. To evaluate the interobserver and intraobserver variability, the intraclass correlation coefficient (ICC) were calculated for each measurement and evaluated by means of ICCs. Dichotomous variables are presented as number (percentage) and compared using $\chi 2$-test. All analysis was done with SPSS version 16.0 (SPSS Inc., Chicago, IL) and two-tailed p-value of <0.05 was considered statistically significant.

RESULTS

A total of 52 patients were enrolled for the current study. According to the current criteria of severe AS, i.e. AVA index<0.6cm^2/m^2, 71% of the patients were severe AS. None of the patients had LV systolic dysfunction, i.e. LV ejection fraction (EF) <50% and all patients were in New York Heart Association class I or II as declared in the Methods. The distribution pattern of native T1 showed a normal distribution (**Figure 4-1A**). Native T1 values showed good correlation with the degree of diffuse myocardial fibrosis, quantified by Picrosirius red staining on intraoperative myocardial biopsy specimens (**Figure 4-1B**).

Thus, the study population was divided into three groups according to the native T1 value. The baseline clinical characteristics of the study population are summarized in Table 1, together with a representative native T1 mapping image of the myocardium in the patients with low and high native T1 value (**Figure 4-2**). In brief, there was no difference in the baseline clinical characteristics between the three groups (**Table 4-1**). However, the dimension of the LV was significantly different between the three groups. Also, the e' velocity was marginally larger in the patients with the lowest native T1 tertile. The severity of AS was significantly different between the three groups, with the highest native T1 tertile group showing the most severe degree of AS. The highest native T1 tertile group also had the worst myocardial contractility assessed by the global longitudinal and circumferential strain. In brief, there was a significant tendency towards

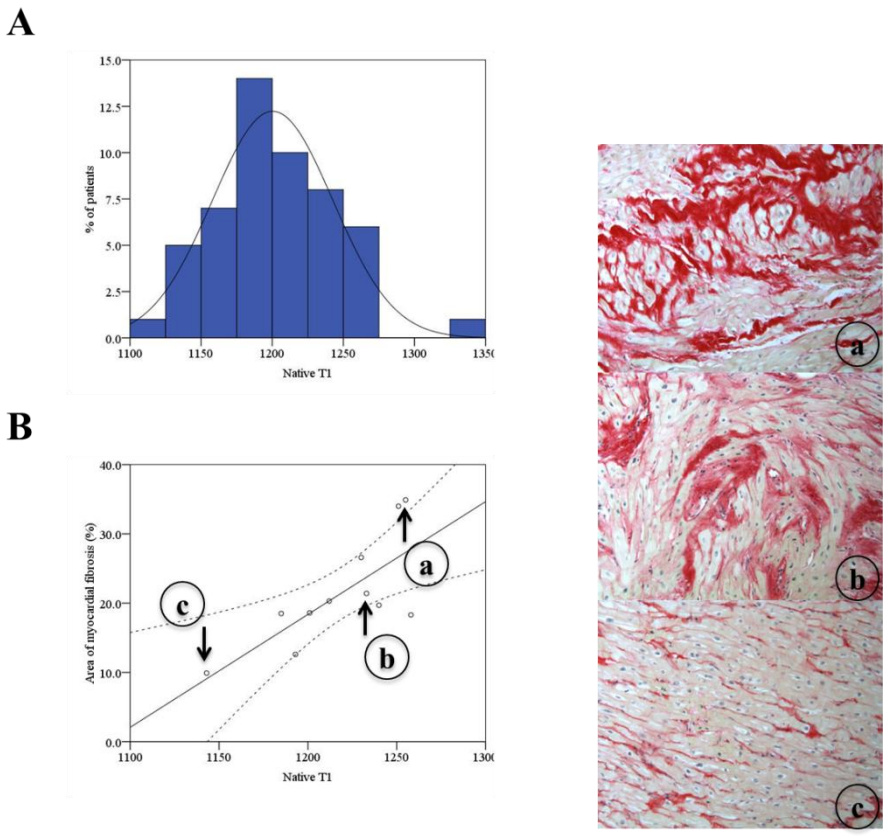

Figure 4-1. Distribution of native T1 value in the study population and its correlation with the degree of diffuse myocardial fibrosis.

(A) The distribution pattern of native T1 value in the study population was drawn by histogram (n=52) and tested for normal distribution. (B) The correlation between native T1 value and the degree of myocardial fibrosis was analyzed. Myocardial specimens were taken during surgical aortic valve replacement from the LV basal septum and stained with Picrosirius red staining. Representative images are shown for each representative degree of myocardial fibrosis (arrows).

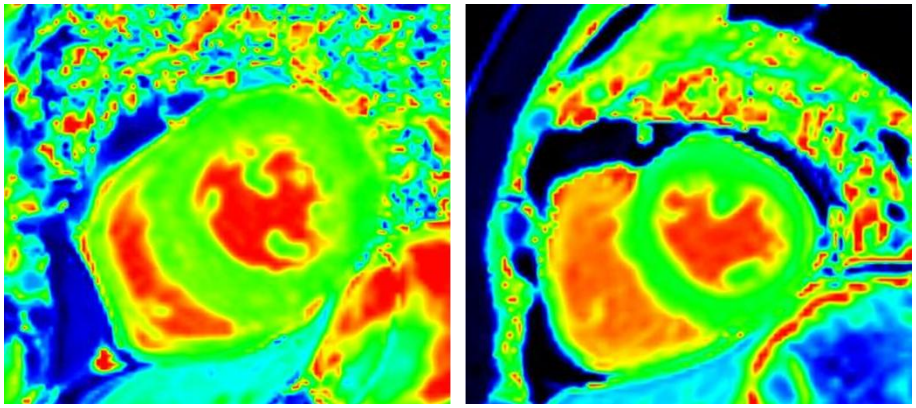

Figure 4-2. Representative images of T1 mapping results of the patients in each group with precontrast T1 value >median and ≤median.

The precontrast T1 was 1306 msec for the patient in the left panel and AVA index 0.31cm^2, mean PG 65mmHg, Vmax 5.1m/sec. The LV mass index was 105 g/m^2 and GLS -12.3%, GCS -16.6%. The precontrast T1 was 1141 msec for the patient in the right panel and AVA index 0.71cm^2, mean PG 24mmHg, Vmax 3.3m/sec. The LV mass index was 62.9 g/m^2 and GLS -17.8%, GCS -18.4%.

	Total (n=52)	Lowest native T1 tertile (n=17)	Middle native T1 tertile (n=17)	Highest native T1 tertile (n=18)	p-value
Male	27 (51.9)	10 (58.8)	7 (41.2)	10 (55.6)	0.547
Hypertension	25 (48.1)	7 (41.2)	11 (64.7)	7 (38.9)	0.245
Diabetes mellitus	12 (23.1)	3 (17.6)	5 (29.4)	4 (22.2)	0.714
Hyperlipidemia	5 (9.6)	3 (17.6)	1 (5.9)	1 (5.6)	0.679
Current smoker	4 (7.7)	1 (5.9)	2 (11.8)	1 (5.6)	0.744
Atrial fibrillation	0	0	0	1 (5.6)	0.382
Age	66 (10)	64 (13)	67 (9)	68 (10)	0.559
BSA (kg/m^2)	1.67 (0.15)	1.66 (0.13)	1.66 (0.15)	1.68 (0.17)	0.926
Serum Cr (mg/dL)	0.88 (0.22)	0.88 (0.19)	0.86 (0.19)	0.89 (0.26)	0.936
Systolic BP (mmHg)	131 (17)	133 (17)	128 (19)	133 (17)	0.659
Diastolic BP (mmHg)	70 (10)	73 (12)	67 (11)	71 (8)	0.279

Table 4-1. Baseline clinical characteristics of the entire study population.

The study population was divided into three groups according to the native T1 value. Continuous variables are presented as mean (standard deviation) and dichotomous variables as number (percentage). The significance of the difference in each parameters were analyzed using either ANOVA or χ2-test as appropriate. BSA, body surface area; Cr, creatinine; BP, blood pressure.

progressed LV remodeling and AS severity measured by echocardiography as the native T1 value increased (**Table 4-2**).

Also, although there was no difference in the LVEF on CMR, the patients with the highest native T1 demonstrated a significantly larger indexed end-diastolic/systolic volume and mass (**Table 4-3**). The volume index of the left atrium also tended to be larger in patients with the highest native T1. Altogether, there was a significant trend towards larger LV volume and mass as the native T1 value increased. The percentage of patients with delayed enhancement was not different between the three groups.

The correlation between native T1 value and parameters of LV remodeling was drawn using bivariate correlation analysis. There was a modest but significant correlation between native T1 value and indexed end-diastolic/systolic volume, mass measured by CMR (**Figure 4-3**). There was a modest degree of relationship between native T1 value and indexed AVA, transaortic mean pressure gradient and maximal velocity, the parameters of AS severity (**Figure 4-4**). Although there was no significant correlation between LVEF by CMR and native T1 value (**Figure 4-3**), the correlation between GLS, GCS and native T1 value was also significant (**Figure 4-5**), demonstrating the possibility of diffuse myocardial fibrosis in decreasing the myocardial contractility. In addition, native T1 value correlated with parameters of LV diastolic function, e' velocity by tissue Doppler echocardiography and calculated LA volume index by CMR (**Figure 4-5**).

To define the interobserver variability of the native T1 value, 14 randomly selected patients were chosen for measurement of the native T1 value by a

	Total (n=52)	Lowest native T1 tertile (n=17)	Middle native T1 tertile (n=17)	Highest native T1 tertile (n=18)	p-value	p-value for trend
LVEDD (mm)	48.5 (5.3)	46.1 (2.8)	47.9 (6.1)	51.3 (5.0)	0.008	0.003
LVESD (mm)	29.7 (4.0)	27.9 (2.3)	29.3 (4.2)	31.8 (4.4)	0.016	0.005
IVST (mm)	11.3 (2.0)	10.6 (1.9)	11.8 (2.5)	11.6 (1.6)	0.199	0.164
PWT (mm)	10.7 (1.6)	10.0 (1.5)	11.1 (1.7)	11.1 (1.5)	0.070	0.045
E velocity (m/sec)	0.72 (0.22)	0.78 (0.25)	0.73 (0.24)	0.65 (0.16)	0.227	0.085
Deceleration time (msec)	250 (75)	238 (77)	259 (89)	253 (61)	0.701	0.565
e' velocity (cm/sec)	4.5 (1.4)	5.2 (1.8)	4.1 (1.1)	4.1 (1.2)	0.048	0.038
Transaortic peak velocity (m/sec)	4.5 (1.4)	4.1 (0.7)	4.6 (0.8)	4.8 (0.9)	0.053	0.019
Transaortic mean PG (mmHg)	49.6 (19.8)	39.4 (14.0)	51.0 (19.5)	57.8 (21.4)	0.018	0.006
AVA (cm^2)	0.82 (0.25)	0.90 (0.22)	0.81 (0.26)	0.76 (0.25)	0.236	0.090
Indexed AVA (cm^2/m^2)	0.49 (0.15)	0.55 (0.14)	0.49 (0.15)	0.45 (0.14)	0.153	0.054
EF by volume (%)	63.6 (5.2)	64.8 (4.3)	62.9 (3.7)	63.1 (7.0)	0.552	0.372
GLS (%)*	-15.0 (3.2)	-16.8 (2.4)	-15.3 (3.0)	-12.9 (2.9)	0.001	<0.001
GCS (%)*	-20.3 (5.1)	-21.5 (4.7)	-21.6 (3.8)	-18.0 (5.9)	0.067	0.047

Table 4-2. Baseline echocardiographic parameters of the entire study population.

The study population was divided into three groups according to the native T1 value and the variables are presented as mean (standard deviation). The significance of the difference in each parameters were analyzed using ANOVA. *, global longitudinal/circumferential strain was analyzed in 50 and 48 patients, respectively. LVEDD/LVESD, left ventricular end-diastolic/systolic diameter; IVST, interventricular septal thickness; PWT, posterior wall thickness; AVA, aortic valve area; EF, ejection fraction; GLS/GCS, global longitudinal/circumferential strain.

	Total (n=52)	Lowest native T1 tertile (n=17)	Middle native T1 tertile (n=17)	Highest native T1 tertile (n=18)	p-value	p-value for trend
LVEDV index (mL/m^2)	92.8 (23.5)	78.4 (10.5)	95.8 (25.5)	103.7 (24.6)	0.004	0.002
LVESV index (mL/m^2)	32.9 (13.1)	27.9 (8.0)	33.7 (15.0)	36.7 (14.3)	0.130	0.047
LVEF (%)	65.1 (8.3)	64.5 (9.2)	65.6 (7.8)	65.2 (8.4)	0.927	0.816
LV cardiac index (mL/m^2)	3.91 (0.99)	3.43 (1.01)	4.16 (0.94)	4.19 (0.84)	0.041	0.027
LV mass index (g/m^2)	92.2 (27.3)	76.3 (15.1)	95.6 (32.9)	104.0 (24.3)	0.007	0.003
LA volume index (mL/m^2)	49.3 (17.3)	41.5 (17.9)	51.1 (10.3)	55.0 (20.1)	0.060	0.022
Heart rate (BPM)	65.8 (7.9)	66.7 (9.9)	66.1 (7.2)	64.6 (6.7)	0.729	0.433
Late gadolinium enhancement	14 (26.9)	6 (35.3)	3 (17.6)	5 (27.8)	0.508	

Table 4-3. Baseline cardiac magnetic resonance parameters of the entire study population.

The study population was divided into three groups according to the native T1 value and the variables are presented as mean (standard deviation) or number (percentage). The significance of the difference in each parameters were analyzed using ANOVA or $\chi 2$-test as appropriate. LVEDV/LVESV, left

ventricular end-diastolic/systolic volume; LVEF, left ventricular ejection fraction; BPM, beats per minute.

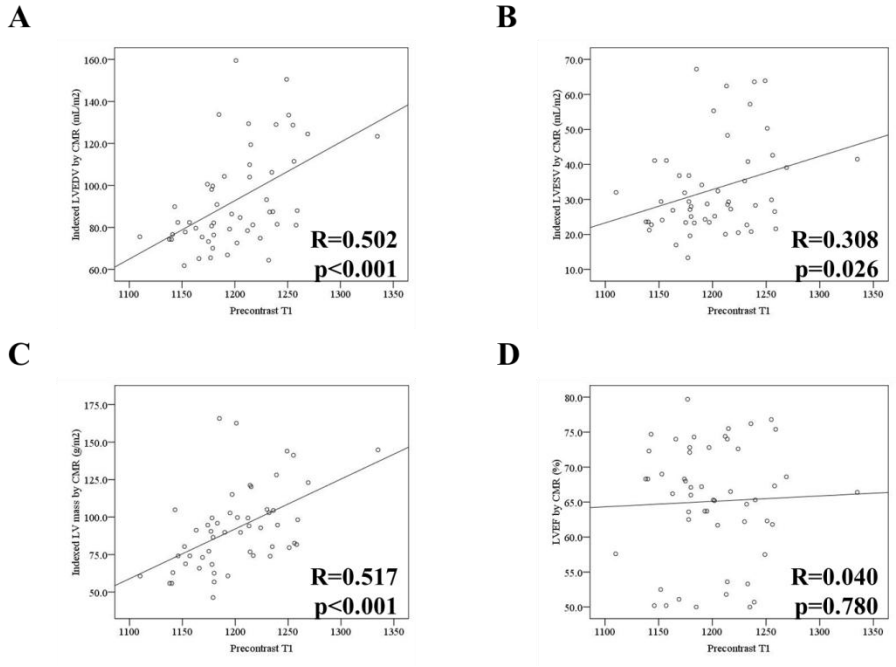

Figure 4-3. Correlation between native T1 value and various LV structural parameters.

Correlation between native T1 value and (A) indexed end-diastolic LV volume, (B) indexed end-systolic LV volume, (C) indexed LV mass and (D) LV ejection fraction measured by CMR was analyzed.

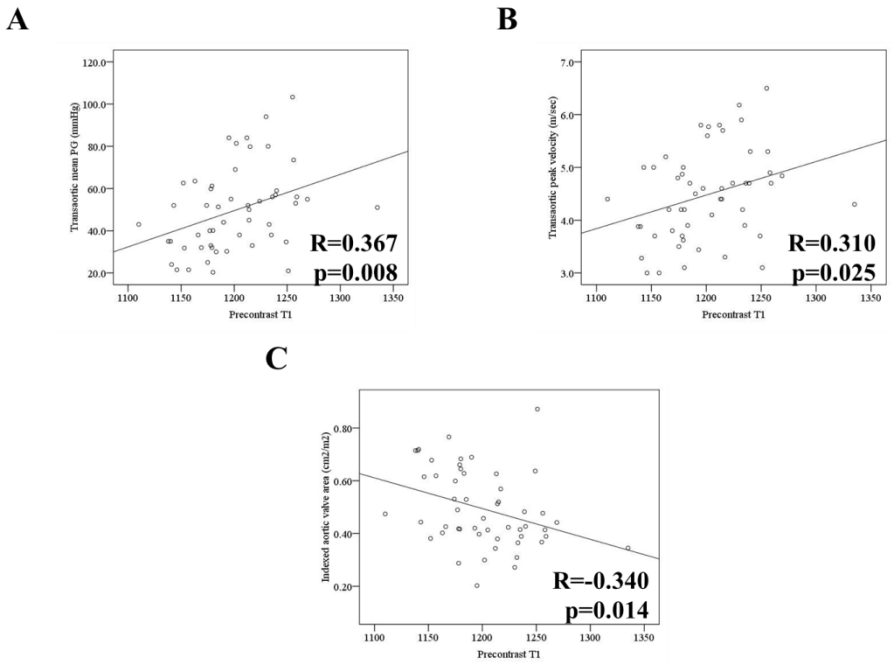

Figure 4-4. Correlation between native T1 value and indices of aortic stenosis severity.

Correlation between native T1 value and various parameters of AS severity, (A) transaortic mean pressure gradient, (B) transaortic peak velocity by continuous wave Doppler imaging, (C) indexed aortic valve area by continuity equation was analyzed.

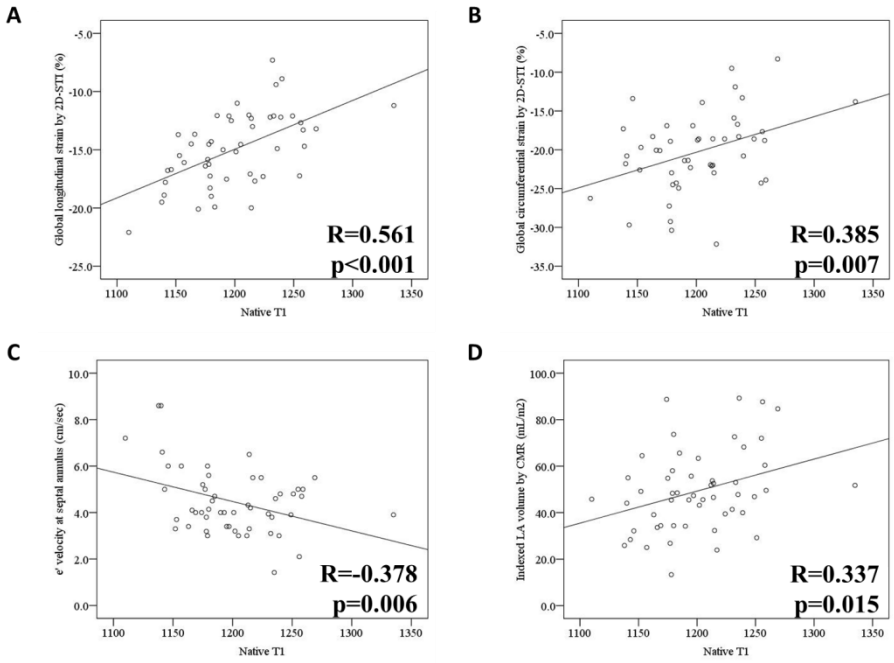

Figure 4-5. Correlation between native T1 value and various LV functional parameters.

Correlation between native T1 value and parameters of LV contractility, (A) global longitudinal strain and (B) global circumferential strain by 2D-speckle tracking imaging, was analyzed. Also, the correlation between native T1 value and parameters of LV diastolic function, (C) e' velocity at the mitral septal annulus by tissue Doppler imaging on echocardiography and (D) indexed LA volume calculated by CMR was analyzed.

observer. The ICC was 0.978 for interobserver variability, indicating excellent interobserver agreement. Also, the same set of patients was reevaluated by the first observer for assessment of intraobserver variability for native T1 values. The ICC was 0.935 for intraobserver variability, again indicating good intraobserver agreement.

DISCUSSION

Following the technical advance of CMR, it has become more and more possible to visualize even the minimal degree of myocardial fibrosis(85). These findings have been verified in various human and animal studies(85), particularly in patients with severe AS as well(18, 19, 43). The presence of LGE on CMR demonstrate worse clinical outcome compared to those without in severe AS patients(18, 19, 43). Furthermore, the presence of focal LGE has also been associated with adverse functional and ventricular remodeling in these patients(18). Altogether the clinical utility and risk stratification using LGE on CMR has been demonstrated in patients with severe AS.

However, from a mechanistic point of view, the myocardium undergoes diffuse interstitial fibrosis rather than focal fibrosis in response to pressure overload(78), which significantly influences LV remodeling in terms of both structure and function(33). The presence of LGE is dependent on a presumptive assignment of 'normal myocardium'(86), which is difficult to characterize exactly on inversion recovery sequence in the setting of diffuse myocardial fibrosis. In other words, there may be no 'normal myocardium' in pressure-loaded ventricle because the entire ventricle may be involved with diffuse fibrosis. Therefore, a different approach is needed for evaluating diffuse myocardial fibrosis(87).

In this report, we have found the following important findings in minimally symptomatic, moderate to severe AS patients. First, the native T1 values reflect the degree of diffuse myocardial fibrosis, as shown by the good

correlation between the degree of fibrosis on histology and native T1 value. Second, based on the first finding, the degree of diffuse myocardial fibrosis measured noninvasively correlates well with the degree of ventricular remodeling and the degree of AS. Third and most importantly, even in patients with minimal symptoms, patients with more diffuse myocardial fibrosis demonstrate a progressed degree of subclinical ventricular remodeling that was not reflected by the symptomatic status of the patient. Collectively, these findings show the effectiveness of a simple and yet, a valuable test for assessing diffuse myocardial fibrosis noninvasively using CMR in AS patients.

Much of the literatures at the current stage have demonstrated the efficacy of post-contrast T1 values and the calculation of extracellular volume fraction from these values for evaluation of the degree of diffuse myocardial fibrosis in AS(55, 88). These techniques have been sharpened recently for more accurate evaluation and have also been simplified to be used more easily. However, up to now, the techniques/sequences need technical expertise and require additional time for evaluation(55). Furthermore, gadolinium contrast is difficult to use in patients with significant renal disease(80), which in turn is an important factor of diffuse myocardial fibrosis and aortic sclerosis.

Recently, the clinical utility of noncontrast T1 has been demonstrated in patients with AS(83). The main findings of the previous paper demonstrated that patients with symptomatic severe AS were more likely to have longer noncontrast T1 value compared to those without symptoms. Our paper is different with the previous paper in that even in patients with no symptoms due to AS, native T1 may reflect and correlate with the degree of subclinical,

adverse ventricular remodeling. Although the current guidelines integrate only symptoms and LVEF for surgical treatment of severe AS(1, 65), several papers have demonstrated that symptoms and LVEF may not be enough to detect early myocardial damage(50). More specifically, several parameters, such as GLS, energy loss index, B-type natriuretic peptide have all been suggested to be integrated as useful adjunct parameters for planning the treatment of severe AS(50). In this aspect, native T1 may be another useful adjunct parameter to detect the subclinical myocardial fibrosis and also, myocardial dysfunction in AS patients.

In our paper, it was interesting to find that CMR was able to discriminate the subtle and yet, significant differences in volume, mass and myocardial contractility between patients with high and low native T1. These findings demonstrate that the degree of diffuse myocardial fibrosis assessed noninvasively by CMR may be a significant determinant of the ventricular function and structure in AS patients. Although it has been demonstrated in patients with depressed LV systolic function or significant symptoms due to severe AS(83), it was alarming to see that this also holds true to patients with no symptoms in our study cohort. It also means that the clinicians dealing with severe AS have advanced into an era that CMR may be integrated to assess the degree of adverse subclinical myocardial fibrosis more accurately and more directly than the past years. This method may be more useful in light of the recent data demonstrating that even asymptomatic severe AS patients have a high event rate(89) and that early surgery in severe AS may warrant a better clinical outcome(32).

Our paper, as in the previous paper, demonstrated that the native T1 value correlates well with the degree of diffuse myocardial fibrosis on histologic examination(83). However, histologic examination is invasive and represents only a piece of the myocardium in the ventricular wall that may not represent the fibrotic status of the whole myocardium. Native T1 mapping using the MOLLI sequence that we have used for the current study represents a reproducible, noninvasive and yet, a simple method for detection of diffuse myocardial fibrosis. If this technique holds true for other types of myocardial disease(79), it may be useful for not only assessing the degree of diffuse myocardial fibrosis but also for predicting the outcome(90) and assessing the treatment response of patients with diffuse myocardial fibrosis.

One also interesting finding was that the difference of LGE incidence between the three groups was not different. However, the findings identified with LGE represents replacement fibrosis, whereas the quantification of T1 mapping represents reactive interstitial fibrosis(77). Although it has been demonstrated that reactive interstitial fibrosis precedes replacement fibrosis(78), this has never been proved thoroughly but has remained in a conceptual status. Moreover, the reactive interstitial fibrosis is a dynamic process that is potentially reversible(58, 76), whereas replacement fibrosis is not. The moderate correlation between the LGE quantification and parameters of LV function, both systolic and diastolic, shown in part 2 also demonstrates that quantification of LGE itself may not be the optimal surrogate for assessing the subclinical myocardial fibrosis and dysfunction, especially in a setting like AS. It may also demonstrate that there is an active, dynamic

process of profibrotic and antifibrotic mechanism that is involved in the presentation of a detectable range of fibrosis, that is LGE.

The current study is not without limitations. First, the sample size was not large and furthermore, the accurate validation of native T1 with the histologic degree of diffuse myocardial fibrosis was assessed in only a subgroup of these patients. However not all of our patients underwent surgery for AS and some of the patients refused myocardial biopsy. Second, we did not analyze other cohort of myocardial disease and whether this technique may hold good for other types of myocardial disease needs more testing and further studies on this issue are to be waited. Third, it remains to be demonstrated whether factors known to influence the myocardial performance in AS, such as diabetes mellitus and sex, do actually affect diffuse myocardial fibrosis in a larger cohort.

In conclusion, we have demonstrated that in asymptomatic patients with moderate to severe AS, native T1 values on CMR reflect the degree of diffuse myocardial fibrosis. Furthermore, assessment of diffuse myocardial fibrosis using MOLLI sequence reflects the degree of subclinical myocardial fibrosis and the structural and functional ventricular remodeling. Our findings warrant a more in-depth and yet, a wider application of this technique in various myocardial diseases in the near future.

REFERENCES

1. Bonow RO, Carabello BA, Kanu C, de Leon AC, Jr., Faxon DP, Freed MD, et al. ACC/AHA 2006 guidelines for the management of patients with valvular heart disease: a report of the American College of Cardiology/American Heart Association Task Force on Practice Guidelines (writing committee to revise the 1998 Guidelines for the Management of Patients With Valvular Heart Disease): developed in collaboration with the Society of Cardiovascular Anesthesiologists: endorsed by the Society for Cardiovascular Angiography and Interventions and the Society of Thoracic Surgeons. Circulation. 2006;114:e84-231.

2. Hachicha Z, Dumesnil JG, Bogaty P, Pibarot P. Paradoxical low-flow, low-gradient severe aortic stenosis despite preserved ejection fraction is associated with higher afterload and reduced survival. Circulation. 2007;115:2856-64.

3. Dumesnil JG, Pibarot P, Carabello B. Paradoxical low flow and/or low gradient severe aortic stenosis despite preserved left ventricular ejection fraction: implications for diagnosis and treatment. Eur Heart J. 2010;31:281-9.

4. Cho GY, Marwick TH, Kim HS, Kim MK, Hong KS, Oh DJ. Global 2-dimensional strain as a new prognosticator in patients with heart failure. J Am Coll Cardiol. 2009;54:618-24.

5. Reant P, Labrousse L, Lafitte S, Bordachar P, Pillois X, Tariosse L, et al. Experimental validation of circumferential, longitudinal, and radial 2-

dimensional strain during dobutamine stress echocardiography in ischemic conditions. J Am Coll Cardiol. 2008;51:149-57.

6. Devereux RB, Reichek N. Echocardiographic determination of left ventricular mass in man. Anatomic validation of the method. Circulation. 1977;55:613-8.

7. Reisner SA, Lysyansky P, Agmon Y, Mutlak D, Lessick J, Friedman Z. Global longitudinal strain: a novel index of left ventricular systolic function. J Am Soc Echocardiogr. 2004;17:630-3.

8. Delgado V, Tops LF, van Bommel RJ, van der Kley F, Marsan NA, Klautz RJ, et al. Strain analysis in patients with severe aortic stenosis and preserved left ventricular ejection fraction undergoing surgical valve replacement. Eur Heart J. 2009;30:3037-47.

9. Lancellotti P, Donal E, Magne J, O'Connor K, Moonen ML, Cosyns B, et al. Impact of global left ventricular afterload on left ventricular function in asymptomatic severe aortic stenosis: a two-dimensional speckle-tracking study. Eur J Echocardiogr. 2010;11:537-43.

10. Mollema SA, Delgado V, Bertini M, Antoni ML, Boersma E, Holman ER, et al. Viability assessment with global left ventricular longitudinal strain predicts recovery of left ventricular function after acute myocardial infarction. Circ Cardiovasc Imaging. 2010;3:15-23.

11. Sjoli B, Orn S, Grenne B, Vartdal T, Smiseth OA, Edvardsen T, et al. Comparison of left ventricular ejection fraction and left ventricular global strain as determinants of infarct size in patients with acute myocardial infarction. J Am Soc Echocardiogr. 2009;22:1232-8.

12. Ng AC, Delgado V, Bertini M, van der Meer RW, Rijzewijk LJ, Shanks M, et al. Findings from left ventricular strain and strain rate imaging in asymptomatic patients with type 2 diabetes mellitus. Am J Cardiol. 2009;104:1398-401.

13. Lancellotti P, Cosyns B, Zacharakis D, Attena E, Van Camp G, Gach O, et al. Importance of left ventricular longitudinal function and functional reserve in patients with degenerative mitral regurgitation: assessment by two-dimensional speckle tracking. J Am Soc Echocardiogr. 2008;21:1331-6.

14. Donal E, Bergerot C, Thibault H, Ernande L, Loufoua J, Augeul L, et al. Influence of afterload on left ventricular radial and longitudinal systolic functions: a two-dimensional strain imaging study. Eur J Echocardiogr. 2009;10:914-21.

15. Kouzu H, Yuda S, Muranaka A, Doi T, Yamamoto H, Shimoshige S, et al. Left Ventricular Hypertrophy Causes Different Changes in Longitudinal, Radial, and Circumferential Mechanics in Patients with Hypertension: A Two-Dimensional Speckle Tracking Study. J Am Soc Echocardiogr. 2010;24:192-9.

16. Galderisi M, Lomoriello VS, Santoro A, Esposito R, Olibet M, Raia R, et al. Differences of myocardial systolic deformation and correlates of diastolic function in competitive rowers and young hypertensives: a speckle-tracking echocardiography study. J Am Soc Echocardiogr. 2010;23:1190-8.

17. Sengupta PP, Korinek J, Belohlavek M, Narula J, Vannan MA, Jahangir A, et al. Left ventricular structure and function: basic science for cardiac imaging. J Am Coll Cardiol. 2006;48:1988-2001.

18. Weidemann F, Herrmann S, Stork S, Niemann M, Frantz S, Lange V, et al. Impact of myocardial fibrosis in patients with symptomatic severe aortic stenosis. Circulation. 2009;120:577-84.

19. Azevedo CF, Nigri M, Higuchi ML, Pomerantzeff PM, Spina GS, Sampaio RO, et al. Prognostic significance of myocardial fibrosis quantification by histopathology and magnetic resonance imaging in patients with severe aortic valve disease. J Am Coll Cardiol. 2010;56:278-87.

20. Cramariuc D, Gerdts E, Davidsen ES, Segadal L, Matre K. Myocardial deformation in aortic valve stenosis: relation to left ventricular geometry. Heart. 2010;96:106-12.

21. Pibarot P, Dumesnil JG. Longitudinal myocardial shortening in aortic stenosis: ready for prime time after 30 years of research? Heart. 2010;96:95-6.

22. Clavel MA, Burwash IG, Mundigler G, Dumesnil JG, Baumgartner H, Bergler-Klein J, et al. Validation of conventional and simplified methods to calculate projected valve area at normal flow rate in patients with low flow, low gradient aortic stenosis: the multicenter TOPAS (True or Pseudo Severe Aortic Stenosis) study. J Am Soc Echocardiogr. 2010;23:380-6.

23. Lancellotti P, Donal E, Magne J, Moonen M, O'Connor K, Daubert JC, et al. Risk stratification in asymptomatic moderate to severe aortic stenosis: the importance of the valvular, arterial and ventricular interplay. Heart. 2010;96:1364-71.

24. Nahum J, Bensaid A, Dussault C, Macron L, Clemence D, Bouhemad B, et al. Impact of longitudinal myocardial deformation on the

prognosis of chronic heart failure patients. Circ Cardiovasc Imaging. 2010;3:249-56.

25. Stanton T, Leano R, Marwick TH. Prediction of all-cause mortality from global longitudinal speckle strain: comparison with ejection fraction and wall motion scoring. Circ Cardiovasc Imaging. 2009;2:356-64.

26. Yu CM, Sanderson JE, Marwick TH, Oh JK. Tissue Doppler imaging a new prognosticator for cardiovascular diseases. J Am Coll Cardiol. 2007;49:1903-14.

27. Cramariuc D, Cioffi G, Rieck AE, Devereux RB, Staal EM, Ray S, et al. Low-flow aortic stenosis in asymptomatic patients: valvular-arterial impedance and systolic function from the SEAS Substudy. JACC Cardiovasc Imaging. 2009;2:390-9.

28. Carasso S, Cohen O, Mutlak D, Adler Z, Lessick J, Reisner SA, et al. Differential effects of afterload on left ventricular long- and short-axis function: insights from a clinical model of patients with aortic valve stenosis undergoing aortic valve replacement. Am Heart J. 2009;158:540-5.

29. Chizner MA, Pearle DL, deLeon AC, Jr. The natural history of aortic stenosis in adults. Am Heart J. 1980;99:419-24.

30. Turina J, Hess O, Sepulcri F, Krayenbuehl HP. Spontaneous course of aortic valve disease. Eur Heart J. 1987;8:471-83.

31. Seo JS, Jang MK, Lee EY, Yun SC, Kim DH, Song JM, et al. Evaluation of left ventricular diastolic function after valve replacement in aortic stenosis using exercise Doppler echocardiography. Circ J. 2012;76:2792-8.

32. Kang DH, Park SJ, Rim JH, Yun SC, Kim DH, Song JM, et al. Early surgery versus conventional treatment in asymptomatic very severe aortic stenosis. Circulation. 2010;121:1502-9.

33. Hein S, Arnon E, Kostin S, Schonburg M, Elsasser A, Polyakova V, et al. Progression from compensated hypertrophy to failure in the pressure-overloaded human heart: structural deterioration and compensatory mechanisms. Circulation. 2003;107:984-91.

34. Heymans S, Schroen B, Vermeersch P, Milting H, Gao F, Kassner A, et al. Increased cardiac expression of tissue inhibitor of metalloproteinase-1 and tissue inhibitor of metalloproteinase-2 is related to cardiac fibrosis and dysfunction in the chronic pressure-overloaded human heart. Circulation. 2005;112:1136-44.

35. Polyakova V, Hein S, Kostin S, Ziegelhoeffer T, Schaper J. Matrix metalloproteinases and their tissue inhibitors in pressure-overloaded human myocardium during heart failure progression. J Am Coll Cardiol. 2004;44:1609-18.

36. Villari B, Vassalli G, Monrad ES, Chiariello M, Turina M, Hess OM. Normalization of diastolic dysfunction in aortic stenosis late after valve replacement. Circulation. 1995;91:2353-8.

37. Falcao-Pires I, Hamdani N, Borbely A, Gavina C, Schalkwijk CG, van der Velden J, et al. Diabetes mellitus worsens diastolic left ventricular dysfunction in aortic stenosis through altered myocardial structure and cardiomyocyte stiffness. Circulation. 2011;124:1151-9.

38. Lee SP, Kim YJ, Kim JH, Park K, Kim KH, Kim HK, et al. Deterioration of myocardial function in paradoxical low-flow severe aortic stenosis: two-dimensional strain analysis. J Am Soc Echocardiogr. 2011;24:976-83.

39. Goncalves A, Marcos-Alberca P, Almeria C, Feltes G, Rodriguez E, Hernandez-Antolin RA, et al. Acute left ventricle diastolic function improvement after transcatheter aortic valve implantation. Eur J Echocardiogr. 2011;12:790-7.

40. Chang SA, Park PW, Sung K, Lee SC, Park SW, Lee YT, et al. Noninvasive estimate of left ventricular filling pressure correlated with early and midterm postoperative cardiovascular events after isolated aortic valve replacement in patients with severe aortic stenosis. J Thorac Cardiovasc Surg. 2010;140:1361-6.

41. Kim RJ, Wu E, Rafael A, Chen EL, Parker MA, Simonetti O, et al. The use of contrast-enhanced magnetic resonance imaging to identify reversible myocardial dysfunction. N Engl J Med. 2000;343:1445-53.

42. Herrmann S, Stork S, Niemann M, Lange V, Strotmann JM, Frantz S, et al. Low-gradient aortic valve stenosis myocardial fibrosis and its influence on function and outcome. J Am Coll Cardiol. 2011;58:402-12.

43. Dweck MR, Joshi S, Murigu T, Alpendurada F, Jabbour A, Melina G, et al. Midwall fibrosis is an independent predictor of mortality in patients with aortic stenosis. J Am Coll Cardiol. 2011;58:1271-9.

44. Lang RM, Bierig M, Devereux RB, Flachskampf FA, Foster E, Pellikka PA, et al. Recommendations for chamber quantification. Eur J Echocardiogr. 2006;7:79-108.

45. Nagueh SF, Mikati I, Kopelen HA, Middleton KJ, Quinones MA, Zoghbi WA. Doppler estimation of left ventricular filling pressure in sinus tachycardia. A new application of tissue doppler imaging. Circulation. 1998;98:1644-50.

46. Redfield MM, Jacobsen SJ, Borlaug BA, Rodeheffer RJ, Kass DA. Age- and gender-related ventricular-vascular stiffening: a community-based study. Circulation. 2005;112:2254-62.

47. Aronow WS, Ahn C, Kronzon I, Nanna M. Prognosis of congestive heart failure in patients aged > or = 62 years with unoperated severe valvular aortic stenosis. Am J Cardiol. 1993;72:846-8.

48. Ozkan A, Kapadia S, Tuzcu M, Marwick TH. Assessment of left ventricular function in aortic stenosis. Nat Rev Cardiol. 2011;8:494-501.

49. Steadman CD, Jerosch-Herold M, Grundy B, Rafelt S, Ng LL, Squire IB, et al. Determinants and functional significance of myocardial perfusion reserve in severe aortic stenosis. JACC Cardiovasc Imaging. 2012;5:182-9.

50. Pibarot P, Dumesnil JG. Improving assessment of aortic stenosis. J Am Coll Cardiol. 2012;60:169-80.

51. Ballo P, Mondillo S, Motto A, Faraguti SA. Left ventricular midwall mechanics in subjects with aortic stenosis and normal systolic chamber function. J Heart Valve Dis. 2006;15:639-50.

52. Orlowska-Baranowska E, Placha G, Gaciong Z, Baranowski R, Zakrzewski D, Michalek P, et al. Influence of ACE I/D genotypes on left ventricular hypertrophy in aortic stenosis: gender-related differences. J Heart Valve Dis. 2004;13:574-81.

53. Dweck MR, Joshi S, Murigu T, Gulati A, Alpendurada F, Jabbour A, et al. Left ventricular remodeling and hypertrophy in patients with aortic stenosis: insights from cardiovascular magnetic resonance. J Cardiovasc Magn Reson. 2012;14:50.

54. Iles L, Pfluger H, Phrommintikul A, Cherayath J, Aksit P, Gupta SN, et al. Evaluation of diffuse myocardial fibrosis in heart failure with cardiac magnetic resonance contrast-enhanced T1 mapping. J Am Coll Cardiol. 2008;52:1574-80.

55. Flett AS, Hayward MP, Ashworth MT, Hansen MS, Taylor AM, Elliott PM, et al. Equilibrium contrast cardiovascular magnetic resonance for the measurement of diffuse myocardial fibrosis: preliminary validation in humans. Circulation. 2010;122:138-44.

56. Freeman RV, Otto CM. Spectrum of calcific aortic valve disease: pathogenesis, disease progression, and treatment strategies. Circulation. 2005;111:3316-26.

57. Otto CM. Valvular aortic stenosis: disease severity and timing of intervention. J Am Coll Cardiol. 2006;47:2141-51.

58. Krayenbuehl HP, Hess OM, Monrad ES, Schneider J, Mall G, Turina M. Left ventricular myocardial structure in aortic valve disease before,

intermediate, and late after aortic valve replacement. Circulation. 1989;79:744-55.

59. Shiojima I, Sato K, Izumiya Y, Schiekofer S, Ito M, Liao R, et al. Disruption of coordinated cardiac hypertrophy and angiogenesis contributes to the transition to heart failure. J Clin Invest. 2005;115:2108-18.

60. Orsinelli DA, Aurigemma GP, Battista S, Krendel S, Gaasch WH. Left ventricular hypertrophy and mortality after aortic valve replacement for aortic stenosis. A high risk subgroup identified by preoperative relative wall thickness. J Am Coll Cardiol. 1993;22:1679-83.

61. Cioffi G, Faggiano P, Vizzardi E, Tarantini L, Cramariuc D, Gerdts E, et al. Prognostic effect of inappropriately high left ventricular mass in asymptomatic severe aortic stenosis. Heart. 2011;97:301-7.

62. Tomanek RJ. Response of the coronary vasculature to myocardial hypertrophy. J Am Coll Cardiol. 1990;15:528-33.

63. Flanagan MF, Aoyagi T, Arnold LW, Maute C, Fujii AM, Currier J, et al. Effects of chronic heparin administration on coronary vascular adaptation to hypertension and ventricular hypertrophy in sheep. Circulation. 1999;100:981-7.

64. Friehs I, Margossian RE, Moran AM, Cao-Danh H, Moses MA, del Nido PJ. Vascular endothelial growth factor delays onset of failure in pressure-overload hypertrophy through matrix metalloproteinase activation and angiogenesis. Basic Res Cardiol. 2006;101:204-13.

65. Bonow RO, Carabello BA, Chatterjee K, de Leon AC, Jr., Faxon DP, Freed MD, et al. ACC/AHA 2006 guidelines for the management of patients

with valvular heart disease: a report of the American College of Cardiology/American Heart Association Task Force on Practice Guidelines (writing Committee to Revise the 1998 guidelines for the management of patients with valvular heart disease) developed in collaboration with the Society of Cardiovascular Anesthesiologists endorsed by the Society for Cardiovascular Angiography and Interventions and the Society of Thoracic Surgeons. J Am Coll Cardiol. 2006;48:e1-148.

66. Ganau A, Devereux RB, Roman MJ, de Simone G, Pickering TG, Saba PS, et al. Patterns of left ventricular hypertrophy and geometric remodeling in essential hypertension. J Am Coll Cardiol. 1992;19:1550-8.

67. De Boer RA, Pinto YM, Van Veldhuisen DJ. The imbalance between oxygen demand and supply as a potential mechanism in the pathophysiology of heart failure: the role of microvascular growth and abnormalities. Microcirculation. 2003;10:113-26.

68. Frey N, Olson EN. Cardiac hypertrophy: the good, the bad, and the ugly. Annu Rev Physiol. 2003;65:45-79.

69. Selvetella G, Hirsch E, Notte A, Tarone G, Lembo G. Adaptive and maladaptive hypertrophic pathways: points of convergence and divergence. Cardiovasc Res. 2004;63:373-80.

70. Adams RH, Alitalo K. Molecular regulation of angiogenesis and lymphangiogenesis. Nat Rev Mol Cell Biol. 2007;8:464-78.

71. Giordano FJ, Gerber HP, Williams SP, VanBruggen N, Bunting S, Ruiz-Lozano P, et al. A cardiac myocyte vascular endothelial growth factor

paracrine pathway is required to maintain cardiac function. Proc Natl Acad Sci U S A. 2001;98:5780-5.

72. Yoon YS, Uchida S, Masuo O, Cejna M, Park JS, Gwon HC, et al. Progressive attenuation of myocardial vascular endothelial growth factor expression is a seminal event in diabetic cardiomyopathy: restoration of microvascular homeostasis and recovery of cardiac function in diabetic cardiomyopathy after replenishment of local vascular endothelial growth factor. Circulation. 2005;111:2073-85.

73. Tomanek RJ, Searls JC, Lachenbruch PA. Quantitative changes in the capillary bed during developing, peak, and stabilized cardiac hypertrophy in the spontaneously hypertensive rat. Circ Res. 1982;51:295-304.

74. Breisch EA, White FC, Nimmo LE, Bloor CM. Cardiac vasculature and flow during pressure-overload hypertrophy. Am J Physiol. 1986;251:H1031-7.

75. Milano AD, Faggian G, Dodonov M, Golia G, Tomezzoli A, Bortolotti U, et al. Prognostic value of myocardial fibrosis in patients with severe aortic valve stenosis. J Thorac Cardiovasc Surg. 2012;144:830-7.

76. Diez J, Querejeta R, Lopez B, Gonzalez A, Larman M, Martinez Ubago JL. Losartan-dependent regression of myocardial fibrosis is associated with reduction of left ventricular chamber stiffness in hypertensive patients. Circulation. 2002;105:2512-7.

77. Mewton N, Liu CY, Croisille P, Bluemke D, Lima JA. Assessment of myocardial fibrosis with cardiovascular magnetic resonance. J Am Coll Cardiol. 2011;57:891-903.

78. Weber KT, Brilla CG. Pathological hypertrophy and cardiac interstitium. Fibrosis and renin-angiotensin-aldosterone system. Circulation. 1991;83:1849-65.

79. Ugander M, Oki AJ, Hsu LY, Kellman P, Greiser A, Aletras AH, et al. Extracellular volume imaging by magnetic resonance imaging provides insights into overt and sub-clinical myocardial pathology. Eur Heart J. 2012;33:1268-78.

80. Rydahl C, Thomsen HS, Marckmann P. High prevalence of nephrogenic systemic fibrosis in chronic renal failure patients exposed to gadodiamide, a gadolinium-containing magnetic resonance contrast agent. Invest Radiol. 2008;43:141-4.

81. Baumgartner H, Hung J, Bermejo J, Chambers JB, Evangelista A, Griffin BP, et al. Echocardiographic assessment of valve stenosis: EAE/ASE recommendations for clinical practice. J Am Soc Echocardiogr. 2009;22:1-23.

82. Messroghli DR, Radjenovic A, Kozerke S, Higgins DM, Sivananthan MU, Ridgway JP. Modified Look-Locker inversion recovery (MOLLI) for high-resolution T1 mapping of the heart. Magn Reson Med. 2004;52:141-6.

83. Bull S, White SK, Piechnik SK, Flett AS, Ferreira VM, Loudon M, et al. Human non-contrast T1 values and correlation with histology in diffuse fibrosis. Heart. 2013;99:932-7.

84. Puntmann VO, Voigt T, Chen Z, Mayr M, Karim R, Rhode K, et al. Native T1 mapping in differentiation of normal myocardium from diffuse

disease in hypertrophic and dilated cardiomyopathy. JACC Cardiovasc Imaging. 2013;6:475-84.

85. Wagner A, Mahrholdt H, Holly TA, Elliott MD, Regenfus M, Parker M, et al. Contrast-enhanced MRI and routine single photon emission computed tomography (SPECT) perfusion imaging for detection of subendocardial myocardial infarcts: an imaging study. Lancet. 2003;361:374-9.

86. Simonetti OP, Kim RJ, Fieno DS, Hillenbrand HB, Wu E, Bundy JM, et al. An improved MR imaging technique for the visualization of myocardial infarction. Radiology. 2001;218:215-23.

87. Dweck MR, Boon NA, Newby DE. Calcific aortic stenosis: a disease of the valve and the myocardium. J Am Coll Cardiol. 2012;60:1854-63.

88. Flett AS, Sado DM, Quarta G, Mirabel M, Pellerin D, Herrey AS, et al. Diffuse myocardial fibrosis in severe aortic stenosis: an equilibrium contrast cardiovascular magnetic resonance study. Eur Heart J Cardiovasc Imaging. 2012;13:819-26.

89. Rosenhek R, Zilberszac R, Schemper M, Czerny M, Mundigler G, Graf S, et al. Natural history of very severe aortic stenosis. Circulation. 2010;121:151-6.

90. Wong TC, Piehler K, Meier CG, Testa SM, Klock AM, Aneizi AA, et al. Association between extracellular matrix expansion quantified by cardiovascular magnetic resonance and short-term mortality. Circulation. 2012;126:1206-16.

국문 초록

서론: 대동맥판 협착증은 전세계 그리고 국내에서도 유병률이 증가하고 있다. 무증상의 심근 손상과 섬유화가 흔하므로 비록 감지하기 힘든 좌심실의 재형성이라도 이를 발견하는 것이 대동맥판 협착증의 과정을 이해하고 증거 기반 치료 가이드라인을 수립하는 데에 중요하다.

방법: 본 논문의 일련의 분석은, 중등도 또는 중증의 대동맥판 협착증 환자들의 전향적인 코호트에 대한 분석이다. 제 1 코호트는 정상 구혈률 중증 대동맥판 협착증 환자로 이루어져 있고 환자들은 역설적 저혈류 대동맥판 협착증의 여부로 나누었다. 좌심실의 종축상/원주상 strain 차이를 두 그룹에서 분석하였다. 제 2 코호트에서는 이면성 심초음파와 더불어 지연조영증강을 포함한 심장 자기공명영상을 획득하였다. 지연조영증강 여부와 구혈률에 따라 구분하여 수축기말 탄성도와 이완기 탄성도를 비롯한 좌심실의 기능과의 관련성을 분석하였다. 제 3 코호트는 정상 구혈률이면서 대동맥판 치환술 도중 심내막 조직검사를 받은 중증 대동맥판 협착증 환자들로 이루어졌다. 조직에 대해 PECAM-1 염색을 시행하여 심근 혈관 밀도와 다양한 심초음파 지표와의 상관관계를 분석하였다. 제 4 코호트는 거의 증상이 없는 정상 구혈률, 중등도 또는 중증의 대동맥판 협착증 환자들로

이루어졌으며 MOLLI 시퀀스를 포함한 심장 자기공명영상을 획득하여 조영증강 전의 T1 값과 좌심실 재형성 지표와의 상관관계를 분석하였다.

결과: 제 1 코호트에서, 정상 혈류 대동맥판 협착증 환자들에 비하여 역설적 저혈률 대동맥판 협착증 환자들은 종축상 strain 이 떨어져 있었고 판막-동맥 저항성으로 대변되는 좌심실 후부하가 종축상 strain 의 유의한 예측 인자로 분석되었다. 제 2 코호트에서, 지연조영증강과 좌심실 수축기능부전 중 하나라도 심장 자기공명영상에서 있으면 구조적, 기능적 재형성/기능 저하가 있는 경향을 보였다. 또한 좌심실구혈률이 정상이라도, 지연조영증강이 있으면 좌심실의 탄성이 떨어지는 경향이 있었다. 제 3 코호트에서, 심근의 혈관 밀도는 좌심실의 수축/이완기능, 비후 정도와 상관관계가 있었으며 좌심실 구조가 더 나빠질수록 혈관의 밀도가 증가하는 경향이 유의하게 관찰되었다. 제 4 코호트에서, 조영증강 전의 T1 수치는 미만성 심근 섬유화 정도를 반영하였다. 또한, 증상이 거의 없음에도 불구하고, 미만성 심근 섬유화가 심한 환자들은 좌심실의 재형성이 더 진행되었음이 관찰되었다.

결론: 정상 구혈률의 대동맥판 협착증 환자들에서도 심초음파의 반점 추적 영상, 심장 자기공명영상의 지연조영증강 및 조영증강전 T1 수치를 이용할 경우 미묘하지만 유의한 좌심실의 구조, 기능적인 재형성을 일찍 발견할 수 있다. 또한 좌심실 구혈률이 저하되기

전까지는 대동맥판 협착증이 더 심해지더라도 혈관 생성의 보상 반응이 있음을 발견할 수 있었다. 이 같은 발견들은 향후 중증 대동맥판 협착증 환자들에서 보다 심도있는 좌심실 재형성 과정에 대한 연구가 필요함을 의미하며 이것이 장기적으로 환자들의 예후와 어떤 관계가 있는지도 더 연구되어야 할 부분이다.

*코호트 1 의 분석 결과는 Journal of the American Society of Echocardiography 에 출판 완료된 내용임 (J Am Soc Echocardiogr. 2011;24(9):976-83.).

주요어: 대동맥판 협착증, 심장 자기공명영상, 심초음파, 심실 재형성, 혈관 신생

학번: 2009-31103

ACKNOWLEDGEMENT

First of all, I would like to express my most sincere thanks to Dr. Seil Oh, my thesis director, for giving me the opportunity and the drive for the PhD thesis. His kind devotion of the time and effort to this thesis should be appreciated. I would also like to thank Dr. Dae-Won Sohn, Yong-Jin Kim and Hyung-Kwan Kim, my mentors in the echocardiography/cardiovascular imaging laboratory, for always inspiring me to this series of work in aortic stenosis and also, for thoughtful and critical discussion in the works I do. It would have been impossible to do these works without their generous support. Thanks to Seon-Jin Kim, RN for her assistance in gathering the echocardiographic data, Tae-Kyung Lee, RN for her help in management of the database. Soo-Jeong Choi, RN and Mi-Kyung Hong were helpful in measurements of the precontrast T1 value and 2D-strain.

I would also like to appreciate the efforts of Dr. Hyuk Ahn, Ki-Bong Kim, Kyung-Hwan Kim and Ho-Young Hwang in the Department of Cardiothoracic Surgery for supporting me to gather this cohort of aortic stenosis patients in Seoul National University Hospital. Especially, the result of cohort 3 is to be celebrated with the above teachers in Cardiothoracic Surgery. Dr. Sung-Ji Park and her colleagues should also be commented for their cooperation in making this cohort bigger, especially the cohort 2. Their devotion to the cohort was most helpful in making these results more significant and more generalizable. Dr. Whal Lee and Eun-Ah Park in the

Department of Radiology were really helpful, not only in the analysis of the CMR database but also helpful in setting the MOLLI sequence and providing fruitful insights into how it works. The results of cohort 2 and 4 were only possible with their cooperation and should be shared with them.

This study was partly supported by a grant of the Korean Health Technology R&D Project (A111457), Ministry for Health, Welfare & Family Affairs, Republic of Korea. I would also like to thank the numerous patients and their families for their generous commitment to the studies. I really do hope that my results would shed light into the understanding of aortic stenosis in the future.

My mum and dad, and also, both mother and father-in-law were always supportive in whatever I did. The persistent encouragement from them was always refreshing. Finally and the most importantly, I would like to thank my beloved family, especially my wife Shinae Kang and my daughter, Eulri and Yeri Lee, for always supporting me. I would like to dedicate this work to our most precious gems.